2011

Experimental Determination of Shielding Requirements for PET Medical Facilities

Bradley Scott Brinkley
University of Alabama at Birmingham

EXPERIMENTAL DETERMINATION OF SHIELDING REQUIREMENTS FOR PET MEDICAL FACILITIES

by

BRADLEY S. BRINKLEY

CLAUDIU T. LUNGU, COMMITTEE CHAIR
ALFRED A. BARTOLUCCI
STEVEN M. BECKER
RIEDAR K. OESTENSTAD
SHARON L. WHITE
MICHAEL V. YESTER

A DISSERTATION

Submitted to the graduate faculty of The University of Alabama at Birmingham,
in partial fulfillment of the requirements for the degree of
Doctor of Public Health

BIRMINGHAM, ALABAMA

2011

EXPERIMENTAL DETERMINATION OF SHIELDING REQUIREMENTS FOR PET MEDICAL FACILITIES

BRADLEY S. BRINKLEY

DOCTOR OF PUBLIC HEALTH

ABSTRACT

Purpose: Shielding considerations are important for designing a positron emission tomography/computed tomography (PET/CT) imaging facility, because of the high energy (511 keV) of electron-positron annihilation photons. Since radiation emitted from patients administered PET radiopharmaceuticals includes lower-energy scattered photons, a given thickness of lead attenuates more of the radiation than it would for a monoenergetic beam of 511 keV photons. A more accurate determination of the effective attenuation coefficient of lead for the spectra of photon energies emitted from PET/CT patients could reduce the shielding requirements necessary to adequately protect public health. In this work, the spectra of energies emitted from 14 patients of different Body Mass Index (BMI) are presented.

Methods: The radiation spectra emitted from adult patients injected with ^{18}F FDG at The Kirklin Clinic PET/CT center were measured through an unleaded wall, and a wall that contains 15.9 mm of lead. The spectra were corrected for radioactive decay time, distance from the patient, detection efficiency of the sodium iodide detector at different energies, and normalized to an injected activity of 15 mCi. The counts were summed to produce a measure of the quantity of transmitted radiation. The shielded wall sums were divided by the unshielded wall sums to determine the radiation transmission factor for each patient.

Results: An effective linear attenuation coefficient of μ_{lead} = 0.226/mm was measured in this work. The results were not significantly affected by differences in patient BMI. For a particular lead shielding thickness, new broad-beam transmission factors calculated using μ_{lead} = 0.226/mm are less than the corresponding broad-beam transmission factors in lead at 511 keV given by American Association of Physicists in Medicine Task Group 108.

Conclusions: Since much of the 511 keV annihilation radiation is scattered in the human body, a spectrum of photon energies interacts with the lead shielding. This results in an increase in the effective attenuation coefficient for lead compared to a monoenergetic beam of 511 keV photons. Because of these effects, current shielding designs for PET/CT imaging facilities using lead shielding may result in safety margins that are higher than originally calculated to adequately protect public health.

Keywords: American Association of Physicists in Medicine Task Group 108, broad-beam transmission factors, scatter radiation, PET, PET/CT, shielding

DEDICATION

I dedicate this dissertation to my wife Kay, and my daughter Taylor. They loved, supported, and encouraged me during the years that I completed this work. They provided me with much importance and purpose to my life which helped me to successfully complete this research project.

ACKNOWLEDGEMENTS

I would like to acknowledge the following individuals who helped me complete this research project:

- Dr. Claudiu T. Lungu, my mentor and academic advisor, for his support, encouragement, and guidance during the years that I completed this work.
- Dr. Michael V. Yester and Dr. Sharon L. White, for suggesting this research project, and for their technical expertise and help in completing this work.
- Dissertation committee members Dr. Steven M. Becker, Dr. R. Kent Oestenstad, and Dr. Alfred A. Bartolucci for their participation, input, comments, and suggestions regarding my dissertation.
- PET Supervisor Tommy J. Mahone, and PET Technologists David H. Stringer and Bobbie D. Jackson, particularly David Stringer, for their very valuable assistance in performing patient spectra measurements at The Kirklin Clinic PET/CT center.
- Max L. Richard, the Assistant Vice-President of the UAB Department of Occupational Health and Safety, for providing me with time to work on this research project, and for his participation in my dissertation committee meetings.
- Dr. Michelle V. Fanucchi, Ms. Cherie D. Hunt, and Ms. Phyllis M. Morris in the Department of Environmental Health Sciences, for their help with performing the administrative requirements necessary for completing my doctoral dissertation.

TABLE OF CONTENTS

Page

LIST OF TABLES

LIST OF FIGURES

LIST OF ABBREVIATIONS

AAPM	American Association of Physicists in Medicine
ANOVA	analysis of variance
BMI	Body Mass Index
cm	centimeters
^{18}F FDG	^{18}F Fluoro-2-deoxyglucose
h	hours
HVL	half-value layer
keV	kiloelectron volt
kVp	kilovoltage peak
MBq	million Becquerel
µSv	microSieverts
mCi	milliCuries
mm	millimeters
mSv	milliSievert
NRC	United States Nuclear Regulatory Commission
e^+e^-	positron-electron
PET	positron emission tomography
PET/CT	positron emission tomography/computed tomography
PMT	photomultiplier tube

m^2	square meters
TKC	The Kirklin Clinic
TVL	tenth-value layer
UAB	University of Alabama at Birmingham

CHAPTER 1

INTRODUCTION

Positron Emission Tomography (PET) is very useful diagnostic tool, particularly for cancer detection. Currently the most common radiopharmaceutical used is ^{18}F Fluoro-2-deoxyglucose (^{18}F FDG), which is a glucose analog and has a radiological half-life of 110 minutes. Other radiopharmaceuticals are also being used with increasing frequency for PET imaging. PET has been available in a number of medical centers for more than 25 years, but its use did not become widespread until about 10 years ago[1]. The number of PET centers is increasing rapidly across the United States. The website for the Academy of Molecular Imaging lists approximately 370 member PET centers in the United States[2]. The power of PET lies in its ability to capture physiologic processes and thereby obtain very important diagnostic information unavailable from high-resolution anatomic images. PET is used for the diagnosis, staging and restaging of many types of cancer, such as non-small cell lung cancer, esophageal cancer, and head and neck cancers.

Shielding Requirements

Shielding requirements are an important consideration in the design of a PET or positron emission tomography/computed tomography (PET/CT) imaging facility, because of the high energy of the 2 photons emitted as a result of positron-electron (e^+e^-) annihila-

tion radiation, which is 511 kiloelectron volts (511 keV). The amount of lead shielding needed can be up to 2.54 cm. The American Association of Physicists in Medicine (AAPM) Task Group 108 provides a comprehensive summary of the issues that need to be considered for adequately shielding PET or PET/CT facilities to adequately protect public health, along with example calculations. The 511-keV photons emitted in three dimensions from patients in PET centers after being dosed with ^{18}F FDG are highly penetrating, thereby potentially exposing members of the general public immediately above, below, and adjacent to PET facilities to amounts of ionizing radiation that can exceed regulatory limits unless adequate shielding is used.

Nuclear Regulatory Commission Dose Limits

Under the federal code of regulations 10 CFR 20, PET/CT facilities must be shielded so that the effective dose equivalent to members of the general public in uncontrolled areas does not exceed 1 milliSievert (mSv)/year. The United States Nuclear Regulatory Commission (NRC) is now considering lowering the annual dose limit for radiation workers from 5 rem to 2 rem per year, and for pregnant radiation workers from 500 mrem to 100 mrem per year. The NRC may also consider lowering annual dose limits for members of the public in the future.

Patient and Point Source Spectra

When patients are injected with PET radiopharmaceuticals, they become sources of scattered photons. The spectrum of radiation from a patient is expected to change significantly compared to a point source of the same activity of ^{18}F in air, with a greater

abundance of lower energy photons emitted from a patient. To determine this, the spectrum needs to be measured and analyzed in detail. The human body absorbs some of the annihilation radiation, and the exposure rate emitted from a patient injected with a PET tracer is reduced compared to a point source, but this is generally taken into account in current calculations. The radiation exposure rate at 1 meter from an unshielded patient is relatively low; however, for a busy PET center, the radiation exposure will exist throughout each business day.

Hypothesis

Due to scatter it is expected that a significant portion of the energies emitted from patients administered ^{18}F FDG are substantially lower than 511 keV, so that the effective shielding of lead is higher than has been generally assumed in shielding calculations. The effective attenuation coefficient is the fraction of photons removed from a beam of gamma or x-rays per unit thickness of shielding material. The null hypothesis is that a significant portion of energies emitted from patients are not substantially lower than 511 keV, and the alternative hypothesis is that a significant portion of energies emitted from patients are substantially lower than 511 keV.

Public Health Significance of the Study

A more accurate determination of the effective attenuation coefficient of lead in a PET/CT medical center could reduce the shielding requirements for PET or PET/CT medical facilities necessary to adequately protect public health. Also, a more accurate determination of the effective attenuation coefficient could be used to demonstrate that

shielding at existing PET/CT medical centers may provide more protection to members of the public than originally thought. The results of this research project can be used to generate more accurate radiation exposure estimates for members of the public located adjacent to PET or PET/CT medical facilities that are shielded with lead. These more accurate radiation exposure estimates can be used to determine if an existing PET or PET/CT medical facility is in compliance with stricter NRC regulatory requirements.

Measurements and Calculations Performed in This Research Project

The spectra of energies emitted from patients injected with ^{18}F FDG were measured to investigate these possible effects. Characterizing the spectra of energies emitted from patients injected with ^{18}F FDG must also take into account possible slight changes with increasing patient thickness, since the amount of radiation scattered by patients will depend on the thickness of the patient. However, measurements of the spectra of energies emitted from patients of different body types need to be performed to determine what effect this might have on the total attenuation in shielding. The study included a range of patients of different Body Mass Index (BMI), where BMI is a person's mass in kilograms divided by his or her height in meters squared[3]. The measurements were used to determine an effective attenuation coefficient of lead for the spectra of photons emitted from patients. Based on this data, new broad-beam transmission factors for lead were calculated and can be used to more accurately estimate radiation exposure to members of the public located adjacent to PET medical facilities.

CHAPTER 2

REVIEW OF LITERATURE

Introduction to PET/CT

The ^{18}F FDG is administered by injection into the bloodstream of the patient and accumulates in the organ or area of the patient's body being examined, where it decays by positron emission. The positron annihilates with an electron, resulting in two 511 keV photons being produced, known as annihilation photons. A PET scanner detects these annihilation photons and with the help of a computer algorithm creates images that offer details on the function of organs and tissues inside the patient's body. The CT part of a PET/CT scanner gives information about the location and structure of organs and tissues inside the patient's body, and is also used for attenuation correction for PET images.

PET imaging studies are less directed toward imaging anatomy and structure, and more concerned with depicting physiologic processes within the patient's body, such as rates of glucose metabolism. Areas of greater intensity, called "hot spots", indicate where large amounts of the radiopharmaceutical have accumulated in the organs and tissues of the patient's body and where there is a high level of metabolic activity[4].

Design and Operation of a PET Scanner

Scintillation crystals attached to photomultiplier tubes are used as annihilation radiation detectors in PET. The scintillation crystals are arranged in rings that encircle the

body of a patient undergoing a PET/CT scan. When a positron interacts with an electron, two 511-keV photons are emitted in nearly opposite directions. When both of the 511-keV annihilation photons interact with detectors, circuitry inside the PET scanner identifies interactions occurring at nearly the same time, a process which is called annihilation coincidence detection. The e^+e^- annihilation is assumed to have occurred along a line connecting the two detectors, called the line of response. The number of coincidences detected along each line of response is stored in the memory of the computer that operates the PET scanner. After data acquisition has been completed, the line of response data is reconstructed to produce cross-sectional images of the radionuclide distribution in the patient[5].

Shielding

Attenuation of radiation incident upon material used for shielding includes both absorption and scattering of the incident radiation by the shielding material. Shielding is used in diagnostic radiology, particle accelerators, and nuclear medicine to reduce radiation exposure to members of the public and workers occupationally exposed to ionizing radiation. The need to utilize shielding, and its type of material (lead, concrete, plastic, etc.), thickness, and location for a particular application, are functions of various factors such as photon energy, number, intensity, and geometry of the sources of radiation, and rate of exposure limits at different locations[6].

Physics of Lead Shielding

When interacting with matter, photons are absorbed, scattered, or penetrate through the matter. Scattering is an interaction with matter which results in a change in direction of a photon or particle from its original trajectory. There are four main types of interactions of photons with matter, the first three of which play a role in lead shielding used in PET/CT medical centers: (a) Rayleigh scattering, (b) Compton scattering, (c) photoelectric absorption, and (d) pair production. Since the minimum energy required for pair production (1,020 keV) is two times higher than the 511 keV of annihilation radiation, pair production plays no role in lead shielding used in PET/CT medical centers[7].

Rayleigh scattering. In Rayleigh scattering, an incident photon interacts with and excites an entire atom, instead of individual electrons as in Compton scattering or the photoelectric effect. This interaction takes place mostly with very low energy x-ray photons (15 to 30 keV). In Rayleigh scattering, a photon is emitted from an atom with the same energy as the incident photon, but in a somewhat different direction. Rayleigh scattering is not a significant effect, because of the high energy of annihilation radiation[7].

Compton scattering. Compton scattering is a significant interaction of 511 keV photons in lead shielding. Compton scattering is most likely to occur between photons and outer shell electrons in atoms. The electron is ejected from the atom, and the photon is scattered with less energy and a change in direction compared to the incident photon. The ejected electron dissipates its kinetic energy in matter in the vicinity of the atom. The Compton scattered photon may pass through the lead shielding without interaction or

may undergo subsequent interactions such as Compton scattering, photoelectric absorption, or Rayleigh scattering[7].

Photoelectric effect. The photoelectric effect is the predominant interaction of photons with lead shielding. In the photoelectric effect, all of the energy of an incident photon is absorbed by one of the atom's electrons, which is then ejected from the atom. As in Compton scattering, the ejected electron dissipates its kinetic energy in the matter in the vicinity of the atom. In order for the photoelectric effect to occur, the energy of the incident photon must be greater than or equal to the binding energy of the electron that is ejected from the atom. For photons whose energies exceed the K-shell (inner electron shell) binding energy, photoelectric interactions with K-shell electrons have the highest probability of occurrence. After a photoelectric interaction with a K-shell electron, the atom is ionized, with an inner shell electron vacancy. An electron cascade from the outer electron shells of the atom to the inner shell occurs in order to fill the electron vacancy in the inner shell. The difference in binding energy between electron shells of the atom is released as either characteristic x-rays or electrons expelled from the electron shells of the atom, which are called Auger electrons[7].

Narrow-Beam and Broad-Beam Geometry

In narrow-beam geometry, the interaction of a collimated source of radiation with shielding material and a detector are such that primarily non-attenuated and non-scattered radiation interacts with the detector. In broad-beam geometry, since a large area is radiated, attenuated radiation may be scattered into the detector, so the apparent radiation at-

tenuation is lower compared to narrow-beam measurement[8]. Many publications have used the "narrow-beam, good geometry" assumptions to estimate attenuation coefficients for lead at 511 keV. If narrow-beam geometry is used, calculations of transmission factors (the fraction of incident radiation transmitted through a barrier) for lead at 511 keV may not provide adequate shielding because they neglect scatter buildup factors, which characterize the additional scatter included with a broad-beam radiation measurement compared to a narrow-beam measurement.

PET or PET/CT Imaging Facility Shielding Requirements

The 511-keV annihilation photon energy is significantly higher than energies typically used in diagnostic radiology, which seldom exceed 140 keV. As the energy of radiation increases, more shielding is needed to reduce radiation exposure levels sufficiently to comply with regulatory requirements. One half-value layer (HVL) of shielding material decreases the measured exposure rate by 50%. HVL thicknesses for lead, concrete, and earth are compared in the following table for 511 keV gamma rays and 150 kilovoltage peak (kVp) x rays[9,3]:

Table 1

Half-Value Layer (HVL) Thicknesses for Lead, Concrete, and Earth

	511 keV photons (cm)	150 kVp x rays (cm)
Lead	0.55	0.03
Concrete	8.5	2.2
Earth	15.4	---

It can be seen that additional thicknesses of lead and/or concrete are needed to properly shield a PET or PET/CT imaging facility compared to a typical diagnostic radiology imaging facility.

The dominant factors that affect the amount of shielding required for PET facilities to meet regulatory requirements are the number of patients imaged per week, the amount of radioactive material administered per patient, the length of time that each patient remains in the medical facility, and the percentage of time the rooms or other areas adjacent to the PET imaging area are occupied, including the floors above and below the PET imaging area[1]. For most locations conservative estimates for a dedicated PET facility are 40 patients imaged per week, 555 million Becquerel (MBq) (15 mCi) of ^{18}F FDG administered per patient, one hour for uptake, and 20-30 minutes of imaging time. A patient preparation room for the uptake of ^{18}F FDG is included in the design of PET facilities and becomes an important area in the shielding requirements for the facility. Patients are instructed to remain quiet in the patient preparation room during the uptake of ^{18}F FDG to give time for the ^{18}F FDG to localize, and not go to the muscles.

Estimation of Transmission Requirements for PET Medical Facilities

Many different attenuation coefficients have been used to estimate shielding requirements for PET medical facilities. Publications have used the narrow-beam, good geometry attenuation coefficients for lead in calculations, which results in a half-value layer of 4.1 millimeters (mm) for lead at 511 keV[1,10]. Broad-beam measurements, which include scattered radiation, have been performed to derive tenth-value layers (TVLs) in order to address the issue of scatter buildup. A tenth-value layer is the amount

of shielding needed to reduce radiation exposure to 10% of its incident exposure. However, even TVLs that are obtained from broad-beam measurements, such as those provided by the National Council on Radiation Protection and Measurements (NCRP)[11], may not correctly estimate shielding requirements for PET medical facilities. AAPM Task Group 108 gives Monte Carlo calculations for broad beam transmission at 511 keV for lead compared to the attenuation values using the NCRP TVLs[1]. According to AAPM Task Group 108, there is a very small difference between the TVL and Monte Carlo results for lead up to a 10 mm thickness. With increasing thickness of lead beyond 10 mm, the TVL overestimates the amount of lead required for shielding as compared to the Monte Carlo calculation.

Patient Attenuation of ^{18}F FDG Annihilation Radiation

Since the human body absorbs some of the annihilation radiation, the dose rate emitted from the patient is reduced by a significant factor. Many papers have been published where direct measurements of annihilation radiation have been made at different orientations from the patient[10,12,13]. In a study by Zeff and Yester[14], radiation exposure was measured at three positions from 64 patients injected with ^{18}F FDG during the uptake period before patients were imaged. Compared with a point source used as an in vitro control, a decrease in exposure was observed due to the distribution of ^{18}F FDG and attenuation of radiation within the bodies of the patients. Based on the average of these results, an effective body absorption factor of 0.36 was recommended by AAPM Task Group 108[1]. A recent publication by Elschot, de Wit, and deJong takes into account the effect of self-absorption on the photon energy spectrum in Monte Carlo calculations, and

a significant reduction in the amount of lead shielding required to produce a TVL of shielding was found. Elschot, de Wit, and deJong found that a TVL of shielding for a PET or PET/CT facility is 13.3 mm of lead, compared to 15.9 mm of lead given by AAPM Task Group 108 Monte Carlo calculations[1,15].

Measuring the Spectra of Energies Emitted From Patients

Spectra measurements for patients administered ^{18}F FDG have not yet been published. There have been some studies published using direct dose rate measurements in clinical practice, but none that measure patient spectra in clinical practice. A major reason why no such studies have been published is because it can be quite difficult to avoid interfering with normal clinical operations while taking patient spectra measurements[15]. This study is the first to provide data on patient spectra measurements.

CHAPTER 3

METHODS AND MATERIALS

A sodium iodide detector was used to measure the energy spectra of radiation emitted from adult patients of different BMI injected with ^{18}F FDG at The Kirklin Clinic PET/CT Center. The spectra were measured after the radiation penetrated through an unleaded wall, and after penetrating through a wall that contains 15.9 mm (5/8 inch)-thick lead. The spectra were corrected for time of radioactive decay, distance from the patient, and the detection efficiency of the sodium iodide detector at different energies. The activities injected into each patient were normalized to an activity of 15 mCi. The counts were summed to produce a quantity of transmitted radiation measured after penetrating through the unleaded wall, and the wall containing 15.9 mm of lead. The sums (count) measured through the shielded wall were divided by the sums measured through the unshielded wall to determine the radiation transmission factor for each patient.

The Kirklin Clinic (TKC) PET/CT Center

The patient spectra measurements were performed at The Kirklin Clinic (TKC) PET/CT Center, which is diagrammed in Figure 1 below[16]. The measurements were performed at 30.5 cm (1 foot) outside of the walls of the inner and outer corridors of the patient preparation room located in the lower right corner of Figure 1. A distance of 30.5

cm (1 foot) was chosen because this is the standard distance from a wall used in radiation shielding calculations.

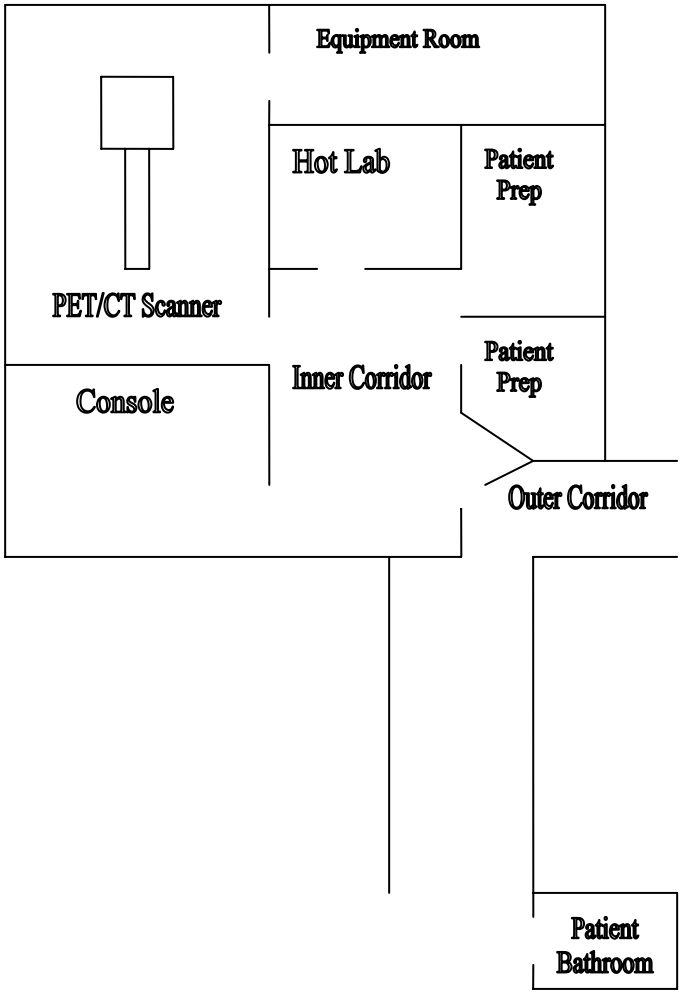

Figure 1. The Kirklin Clinic (TKC) PET/CT Center.

Measuring Patient Spectra

The PET/CT scanner used for imaging patients in the TKC PET Imaging Area is depicted in Figure 2 below.

Figure 2. TKC PET/CT Scanner Used for Imaging Patients.

When measurements were performed of the spectra emitted from a patient, he or she was reclining or sitting quietly in the chair in the patient prep room, which is depicted in Figure 3 below. The patient is instructed to remain quiet in order to avoid metabolizing too much of the FDG in muscles. Observations were made of the approximate angle that the patient was reclined in the chair. (No attempt was made to measure the angle with any degree of precision.) The angle of patient reclining in the chair was not a control variable in this research project; the patient was not instructed to recline any particular amount in the chair.

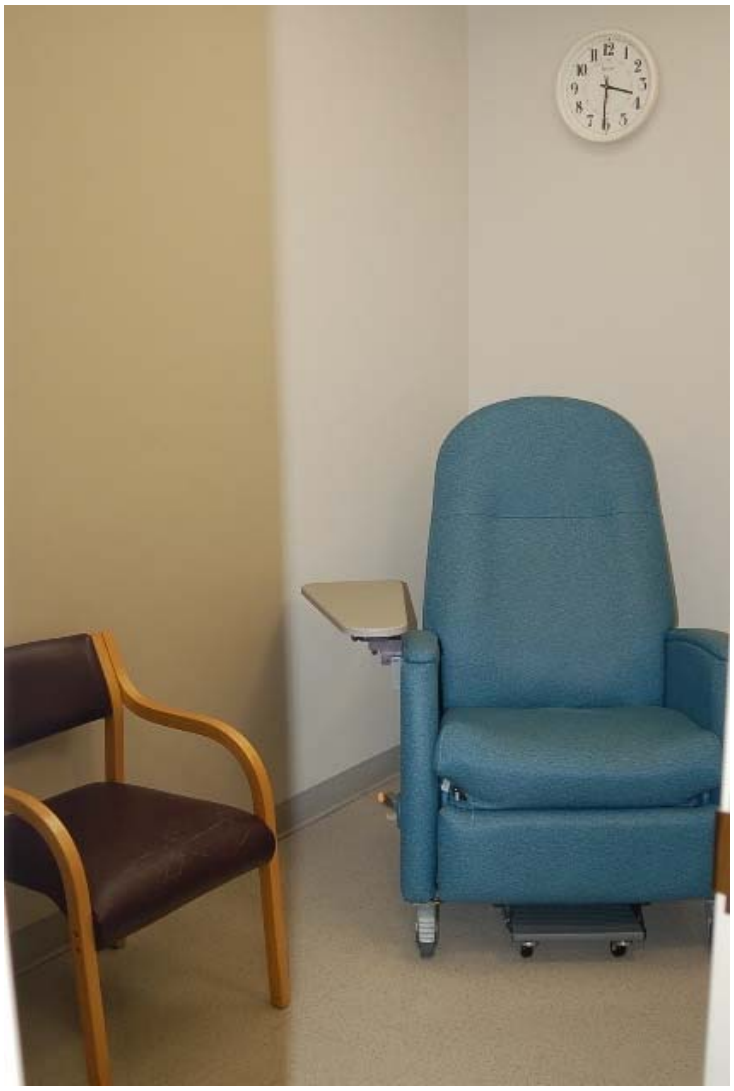

Figure 3. Patient Prep Room in TKC PET/CT Center Adjacent to the Outer Corridor.

Selection of Study Sample

Whenever measurements of the spectra emitted from patients were performed, the last patient of the day at TKC was measured, in order to avoid additional radiation from other patients. Only adult ($\geq$ 19 years old) patients were measured in this study. Expedited IRB approval was obtained in this study for making measurements of patients. Verbal consent was obtained from the patients, and the patient was offered a research in-

formation sheet that described the study. Four of the patients that were measured were in the BMI category Normal Weight (BMI $\leq$ 24.9), five of the patients were in the BMI category Overweight (25.0 $\leq$ BMI $\leq$ 29.9), and five of the patients were in the BMI category Obese (BMI $\geq$ 30.0).

Patient Measurement Difficulties. The reason a much larger patient population was not chosen was because there were many problems encountered in measuring patients. Only the last patient of the day at The Kirklin Clinic PET/CT Center could be measured, which obviously limited patient measurements to no more than one per day. Sometimes the PET/CT scanner required maintenance, which made taking patient measurements impossible. One day the equipment was set up and ready to take measurements, but the patient could not be dosed. Also, it was rather difficult at times to avoid interfering with normal clinical operations while taking patient measurements.

Radiation Spectra Measuring Equipment

Sodium Iodide Detector

A sodium iodide detector with a multi-channel analyzer was used to measure energy spectra for ^{18}F in these experiments. The basic components of a photomultiplier tube (PMT) are illustrated in Figure 4[17].

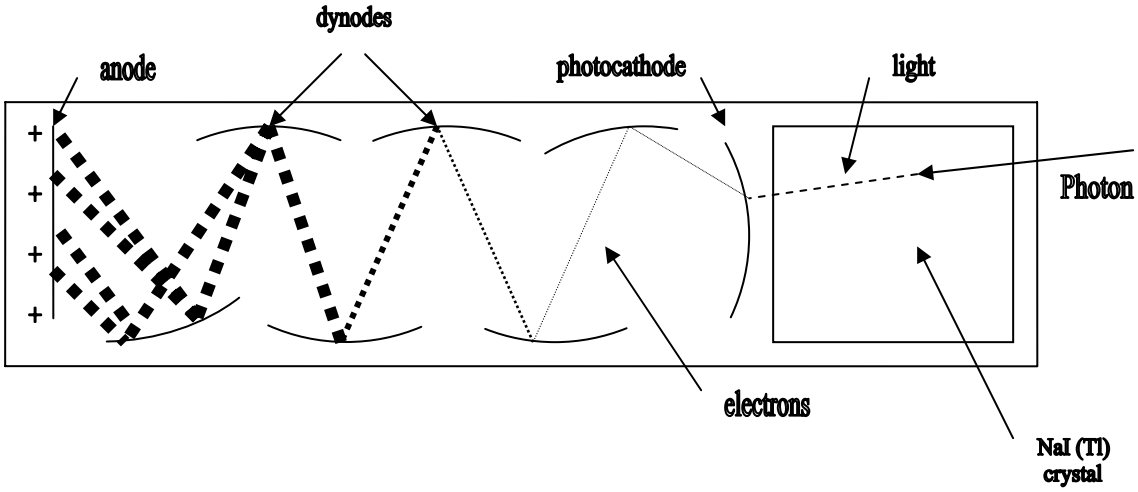

Figure 4. Photomultiplier Tube Operation.

The sodium iodide crystal converts energy from radiation deposited in the scintillation medium into light (UV or visible) flashes or scintillations. The brightness of the light scintillation is proportional to the energy deposited by the incident radiation in the scintillation medium. The PMT converts the scintillation into electrical pulses which vary in pulse height according to the energy of the radiation incident on the crystal. This proportionality relationship permits energy discrimination capabilities with the sodium iodide crystal. These electrical pulses are then sorted with the multi-channel analyzer based on the energy of the radiation they represent.

Scintillation Counter Components

The basic components of a scintillation counter are illustrated below in Figure 5[17].

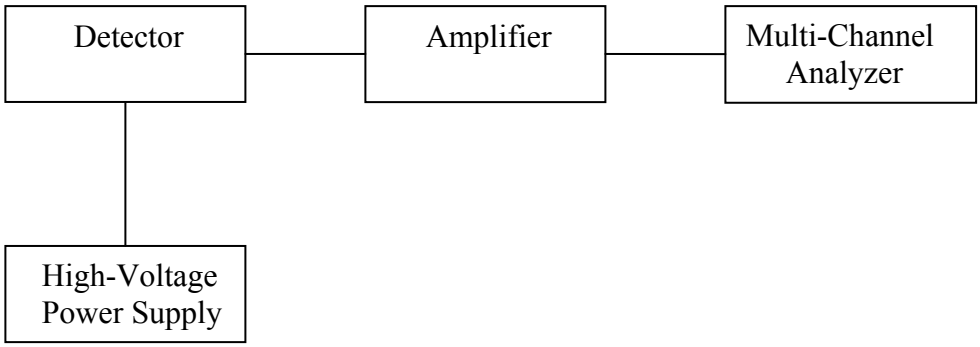

Figure 5. Basic Scintillation Counter Components.

The high voltage power supply provides voltage for operation of the PMT. The amplifier shapes and amplifies the pulses from the PMT, which increases the signal-to-noise ratio of the pulses. The multi-channel analyzer sorts electrical pulses coming from the amplifier by their pulse heights. The multi-channel analyzer used in this work has 256 channels. Each channel has an energy range of slightly more than 4 keV. The multi-channel analyzer records the number of counts in each channel while a spectrum is being measured. A spectrum is generated from the number of counts stored in each channel of the multi-channel analyzer when data is being acquired[18], from approximately 21 keV to approximately 685 keV.

Sodium Iodide Detector and High-Voltage Power Supply

In Figure 6 below, the sodium iodide detector is on the left, and the high-voltage power supply is on the right.

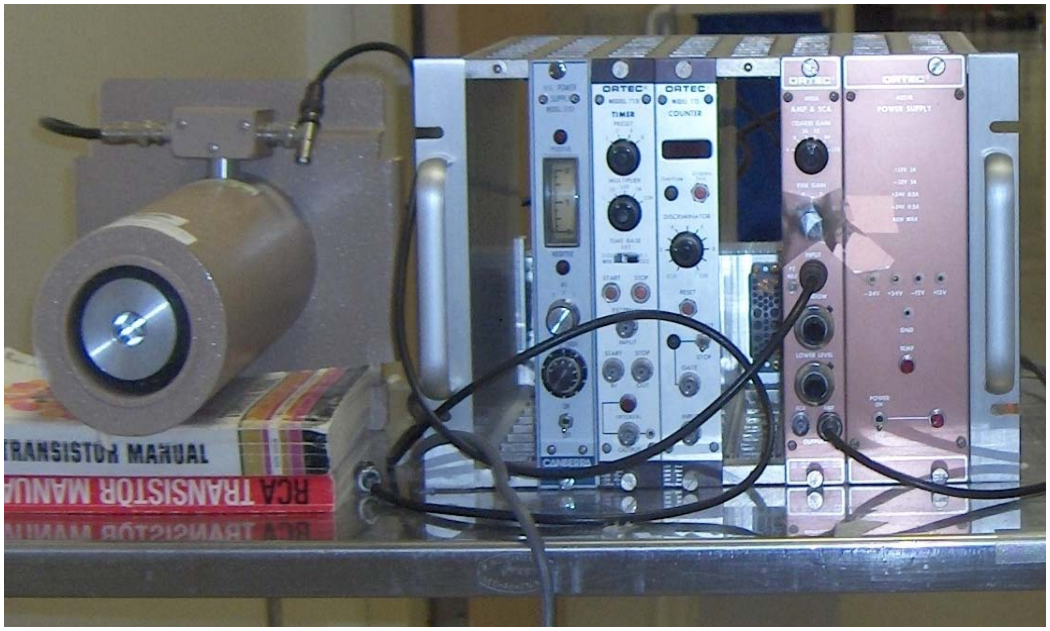

Figure 6. Equipment Used for Taking Measurements of Spectra.

Measuring the Spectra Emitted From Patients, Phantom, and Point Source

Measurements were made for patients of different BMI in order to determine how the spectra of energies emitted from patients differs from the spectra of energies emitted from a point source of ^{18}F, and also to determine how the spectra of energies emitted from patients varies between patients of different BMI. Measurements were also made of ^{18}F measured after being mixed with the water inside an elliptical water-filled phantom, in order to determine if the phantom could be used to simulate adult patients. In some instances it is preferable to measure a phantom instead of patients because a phantom is much more practical and convenient for performing measurements. For instance, phantom measurements do not require IRB approval and patient consent, and can be performed anytime. However, patient measurements are needed to validate phantom measurements.

Patient Spectra Measurements

The spectra emitted from 14 patients were measured after penetrating through the inner corridor wall, which does not contain lead, and also after penetrating through the outer corridor wall, which contains 15.9 mm (5/8 inch)-thick lead. The sodium iodide detector was calibrated with ^{133}Ba, ^{137}Cs, ^{18}F, and ^{99m}Tc each day that spectra were measured, because the response of the amplifier and other electronic components may drift from day to day. The energy calibration data were used to determine the energies in keV of the channels for each patient measurement. The spectrum emitted from a patient was measured for two minutes for each leaded wall measurement, and one minute for each unleaded wall measurement. The times were different because there were far fewer counts per second penetrating through the leaded wall compared to the unleaded wall. The data from the measurements were downloaded into the computer and stored in an Excel spreadsheet format. Background readings were subtracted from each spectrum measurement, and the results were converted to counts per second. The net counts per second were decay-corrected and normalized to an injected activity of 15 mCi, and were corrected for the efficiency of the sodium iodide detector. The results were normalized to a fixed distance (117.2 cm or 46.1 inches) from the patient to the entrance of the sodium iodide detector, so that ratios could be taken of outer corridor to inner corridor measurements for each patient. The fixed distance of 117.2 cm or 46.1 inches was chosen because this is the shortest distance from the entrance of the sodium iodide detector to the center of the chair in the patient prep room that was used for taking patient measurements. The counts per second were summed over the channels of the multi-channel analyzer from approximately 21 keV to approximately 685 keV to obtain the total counts per

second for each patient spectrum. The sum of the counts per second of a spectrum measurement performed without lead shielding in the inner corridor is (N_0), and (N) is the sum of the counts per second of a spectrum measurement performed with lead shielding in the outer corridor.

Measuring Phantom and Point Source Spectra

Phantom spectra. A series of measurements were made of the spectra emitted from the phantom after penetrating through the leaded and unleaded walls. A phantom is a device that is designed to be roughly the same size and shape of an individual, or part of an individual, and to have approximately the same radiation attenuation and scatter characteristics of the human body. The elliptical water-filled phantom used in this research project has roughly the size and shape of a cross-section of the abdomen of an adult person. The phantom is manufactured out of lucite, and is filled with water. When measurements were performed, ^{18}F was mixed with water inside the phantom. Water and lucite have approximately the same radiation attenuation characteristics as the human body. When measurements were made, the phantom was placed on the chair, and raised to the approximate height of the mid-torso of a person sitting in the chair, as illustrated in Figure 7 below.

Figure 7. The Phantom on the Chair Located in the Patient Prep Room.

A closer view of the phantom that was used for this series of measurements is shown in Figure 8 below.

Figure 8. A Closer View of the Phantom.

These measurements of the spectra emitted from the phantom were summed for the channels of the multi-channel analyzer from approximately 21 keV to approximately 685 keV to obtain the total counts per second corrected for background, efficiency, decay, and distance, for each phantom spectrum in a manner very similar to how the spectra emitted from patients were measured and analyzed as described earlier.

Point source spectra. Measurements were made of the spectra emitted from a point source of ^{18}F after penetrating through the unleaded inner corridor wall in order to compare patient spectra attenuation and scatter to point source attenuation and scatter. When measurements were made, the point source was taped to the back of the chair. These measurements of the spectra emitted from the point source were summed for the

channels of the multi-channel analyzer from approximately 21 keV to approximately 685 keV to obtain the total counts per second corrected for background, efficiency, decay, and distance, for each point source spectrum in a manner very similar to how the spectra emitted from patients were measured and analyzed as described earlier.

Ionization Chamber Survey Meter Patient Measurements

Patient exposure rate readings were made using an ionization chamber survey meter in order to check and validate the patient spectra measurements. The patient exposure rate readings were measured using the same geometry as the corresponding spectra measurements for each patient, so that the transmission factors through 15.9 mm (5/8 inch)-thick lead for the patient spectra and the ionization chamber survey meter measurements could be directly compared. At least 10 exposure rate readings were made to obtain an average exposure rate reading for the inner and outer corridor for each patient. A standard background measurement was subtracted from each average patient exposure rate reading. Each average patient exposure rate reading was then corrected for time of radioactive decay, and was normalized to the same fixed distance that was used for the measurements of the spectra emitted from patients (117.2 cm or 46.1 inches).

Determining Detection Efficiency of the Sodium Iodide Detector

The detection efficiency of the sodium iodide detector was needed. The detector efficiency varies as a function of energy. The spectra of photon energies emitted from various radioisotopes (^{241}Am, ^{137}Cs, ^{18}F, and ^{99m}Tc) were measured in air at distances of 61.0 mm (2 feet) and 121.9 mm (4 feet) from the entrance of the sodium iodide detector.

The measurements of the spectra were corrected for geometric efficiency and radioactive decay, and were then used to obtain the efficiency curve for the sodium iodide detector at different energies. The detection efficiency measurements at energies less than or equal to approximately 59 keV were fitted to the linear equation given below on the left side of Figure 9. The detection efficiency measurements at energies greater than or equal to approximately 59 keV were fitted to the linear equation given below on the right side of Figure 9. These two linear equations were used to correct for sodium iodide detector efficiency for the patient, phantom, and point source spectra measurements, for energies from approximately 21 keV to approximately 685 keV.

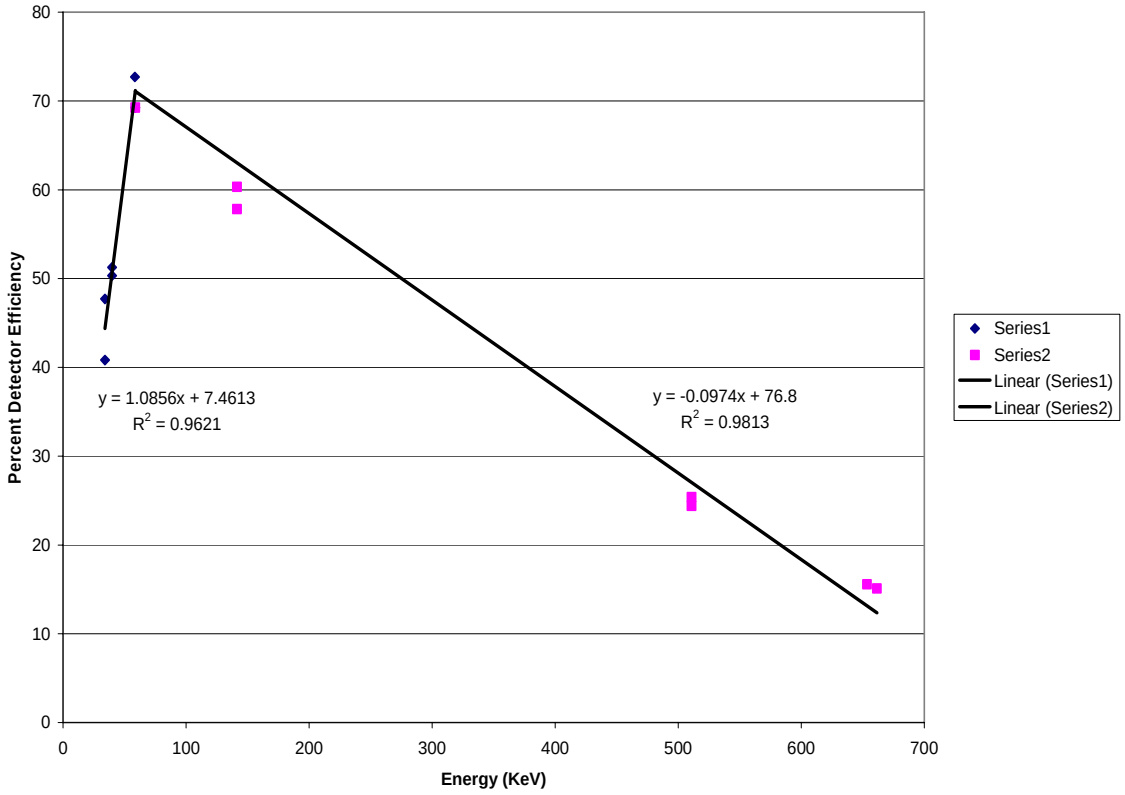

Figure 9. Sodium Iodide Detector Efficiency at Different Energies.

Determination of Measurement Points

Outer Corridor Measurement Point

Some PET/CT medical centers use up to 25.4 mm (1 inch)-thick lead shielding, up to 213.4 cm (7 feet) above the floor, which can create a serious problem with floor loading. Some PET/CT medical centers also add lead to concrete ceilings and floors, which adds to the difficulty of constructing a PET/CT medical center. The Kirklin Clinic PET/CT Center has 15.9 mm (5/8 inch)-thick lead shielding in the wall facing the outer corridor. The lead shielding is composed of sections of lead 30.5 cm (1 foot) wide. The 30.5 cm-wide lead sections are connected by 7.62 cm (3 inch)-wide lead strips which are 15.9 mm (5/8 inches) thick. The left side of Figure 10 below shows the lead in the outer corridor wall under construction, and the right side of Figure 10 shows a close-up view of the lead strips in the wall.

Figure 10. Two Views of the Lead Shielding in the Outer Corridor Wall.

Point source and phantom measurements. Several point source measurements were performed to find the optimal measurement point in the outer corridor. This measurement point was located approximately in the center of one of the 30.5 cm (1 foot)-wide lead sections, equidistant from two of the 7.62 cm (3 inch)-wide lead strips connecting the 30.5 cm-wide lead sections together. This point was chosen to avoid the 7.62 cm-wide lead strips as much as possible, since this would double the amount of lead attenuating the radiation in a localized region. These point source measurements are shown below in Figure 11.

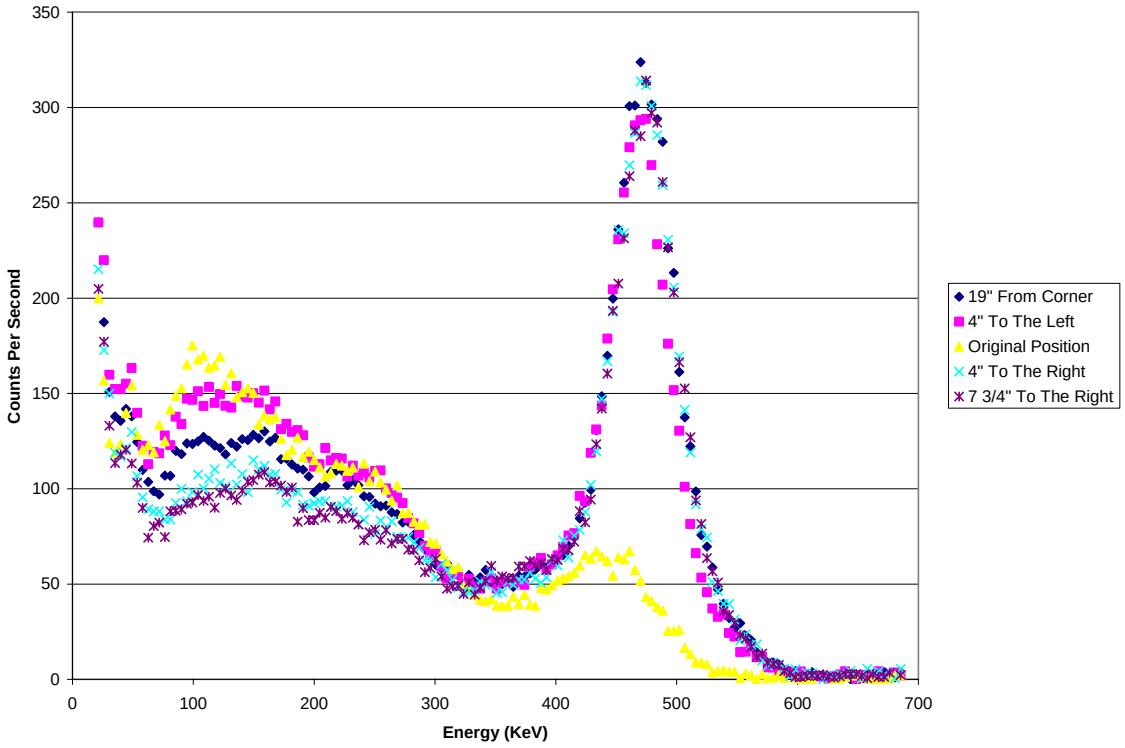

Figure 11. Outer Corridor Point Source Spectra.

To determine this point, the sodium iodide detector was moved to the left and to the right along the outer corridor leaded wall, with the point source taped to the back of the chair in the patient preparation room, and measurements were taken. The measurement results were used to observe the change in transmission factors at different lateral locations in the outer corridor, and thus locate the center of one of the 30.5 cm-wide lead sections. As can be seen in Figure 11 above, a 7.62 cm-wide lead strip was located at "Original Position", since the amount of 511-keV radiation attenuation at that point was greatly increased.

To verify the optimal measurement point, the sodium iodide detector was moved to the left and to the right along the outer corridor leaded wall, with the phantom located in the chair in the patient preparation room, and measurements were taken. The transmission factors did not change significantly at different lateral locations in the outer corridor, and thus the measurement point was located at or near the center of one of the 30.5 cm-wide lead sections. These phantom measurements are shown below in Figure 12.

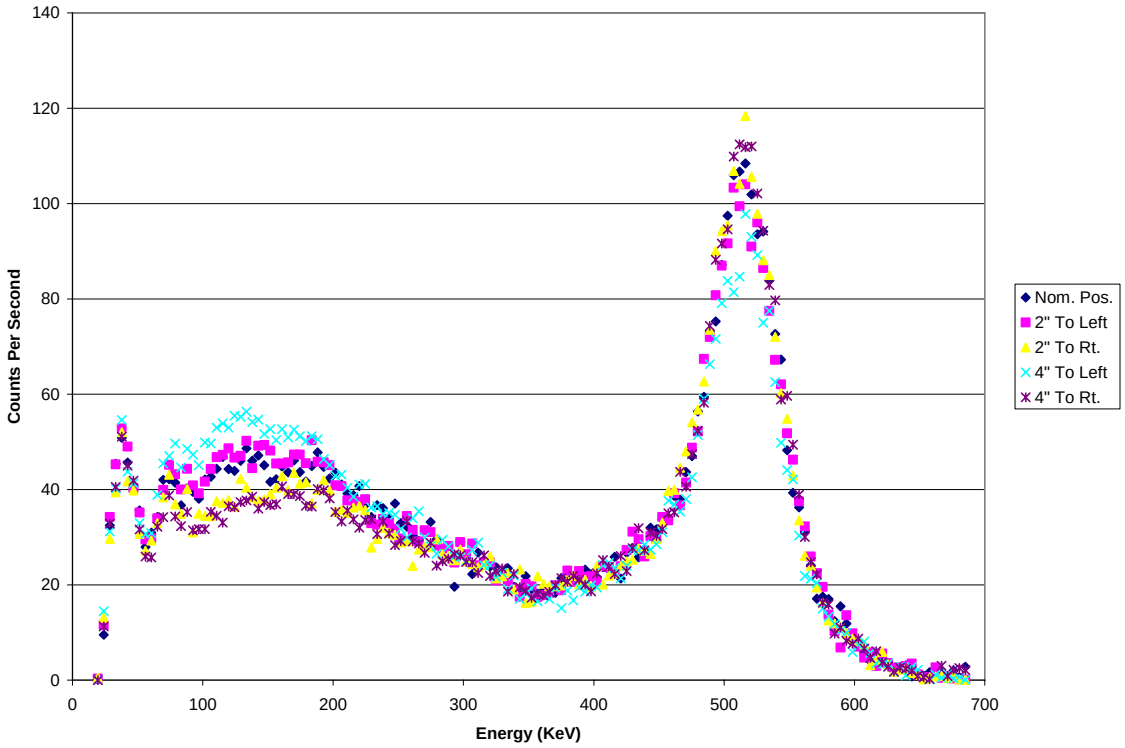

Figure 12. Outer Corridor Phantom Spectra.

Chair position. The chair was located in the patient preparation room with the center of the patient in the chair directly opposite the outer corridor wall measurement point. This position was chosen so that radiation emitted from a patient would strike the outer corridor wall at as small an angle as possible, in order to minimize the effective thickness of the lead shielding. The center of the patient was located approximately 132.1 cm (52 inches) from the outer corridor measurement point 30.5 cm (1 foot) from the wall.

Inner Corridor Measurement Point

The inner corridor wall does not contain lead shielding. Ideally measurements would have been taken directly opposite the center of the patient in the chair in the patient preparation room, but there was not enough room for the equipment in the patient preparation room to take measurements. Also, taking measurements in the patient preparation room would have interfered with patient privacy. Ultimately a measurement point was selected 30.5 cm (1 foot) from the inner corridor wall which was approximately 43.2 cm (17 inches) to the left of directly opposite the center of the patient in the chair in the patient preparation room, at a distance of approximately 180.3 cm (71 inches) from the center of the patient. The distance of 180.3 cm (71 inches) was also chosen to avoid swamping the sodium iodide detector with more counts per second than the detector could distinctly process because of dead time[19]. The inner and outer corridor measurement points are shown below in Figure 13.

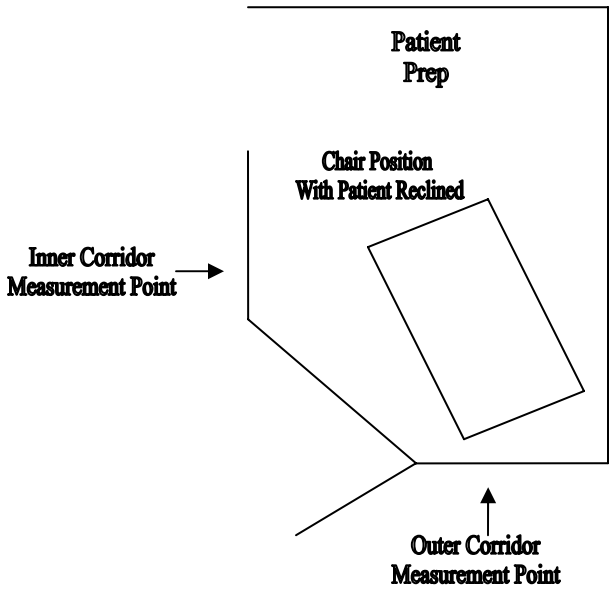

Figure 13. Inner and Outer Corridor Measurement Points.

Calculations

Transmission Factors

The transmission factors (ratios) for the 5/8 inch-thick lead shielding (B_{lead}) in the outer corridor wall of The Kirklin Clinic PET/CT Center for the patient and phantom spectra measurements were calculated using the following equation[20]:

$$B_{lead} = \frac{N}{N_0} \qquad (1)$$

For the ionization chamber survey meter, for each patient, the average exposure rate reading in the outer corridor was divided by the corresponding average inner corridor patient exposure rate reading to calculate the transmission factor.

Statistical Analyses of Patient and Phantom Measurements

The data from measurements were statistically analyzed to determine if the average patient transmission factors (ratios) in each of the three BMI categories (Normal Weight, Overweight, and Obese), and in each of three angle categories of patients reclining in the chair in the patient preparation room (≤ 40 degrees, 40 degrees < angle ≤ 45 degrees, and > 45 degrees), were significantly different. The data were also statistically analyzed to determine if the average patient ratios in each of the three BMI categories were significantly different from the average phantom ratio.

ANOVA. For the statistical analyses of the data, a one-way analysis of variance (ANOVA) was performed on the patient and phantom measurements using a data analysis program in the 2003 version of Microsoft Excel. The one-way ANOVA statistical test

compares the average of two or more groups of data based on one independent variable (or factor). With a one-way ANOVA test it is assumed that the dependent variable is normally distributed, and that the two or more groups have approximately equal variance on the dependent variable. For a one-way ANOVA test, the null hypothesis is that there are no statistically significant differences between the groups' average values, and the alternative hypothesis is that there is a statistically significant difference between the groups' average values (ratios in this case). If the probability value (p-value) generated by the one-way ANOVA test is less than 0.05, there is a statistically significant difference between the average ratios. If the p-value is greater than 0.05, we cannot reject the null hypothesis that there are no statistically significant differences between the average ratios for the groups (patient BMI's, patient reclining angles, and phantom[21].)

New Broad-Beam Transmission Factors for Different Thicknesses of Lead

The value of the effective linear attenuation coefficient (μ_{lead}) was calculated with the following equation[20]:

$$\mu_{lead} = \frac{-\ln(B_{lead})}{(15.9 \text{ mm}),} \qquad (2)$$

where (15.9 mm) is the thickness of the lead shielding in the outer corridor wall. The value of the effective linear attenuation coefficient (μ_{lead}) was multiplied by different thicknesses of lead to obtain new broad-beam transmission factors for different thicknesses of lead at 511 keV using the following equation[20]:

$$B_{lead} = \exp\{(-\mu_{lead}) \times (x)\}, \qquad (3)$$

where (x) is the thickness of the lead.

Transmission Factors for Uncontrolled Areas

Equation 3 gives calculated values for new broad-beam transmission factors for different thicknesses of lead at 511 keV using the experimentally measured value of the effective linear attenuation coefficient (μ_{lead}). The following accepted equation can be used to calculate the maximum transmission factors necessary to meet current regulatory requirements for uncontrolled (B_U) areas located adjacent to a patient preparation room for the uptake of ^{18}F FDG[1]. Below is equation 4, which is used later for example calculations:

$$B_U = 218 \times d^2 \div [T \times N_W \times A_0\,(\text{MBq}) \times t_U\,(h) \times R_{tU}], \text{ where} \quad (4)$$

d^2 = Squared distance from source to barrier in square meters (m^2),

T = Occupancy Factor (an estimate of the fraction of time that a particular individual will occupy an uncontrolled area whenever patients are being injected with ^{18}F FDG during a week[20]),

N_W = Number of patients per week,

A_0 = Administered Activity in million Becquerel (MBq),

$t_U\,(h)$ = Uptake time of ^{18}F FDG in hours (h), and

R_{tU} = Dose reduction factor due to decay of ^{18}F FDG over uptake time t.

CHAPTER 4

RESULTS

Patient Spectra Plots

Figure 14 below shows the spectra emitted from three adult patients administered ^{18}F FDG normalized to 15 mCi, measured after penetrating through the wall in the outer corridor which contains 15.9 mm (5/8 inch) of lead.

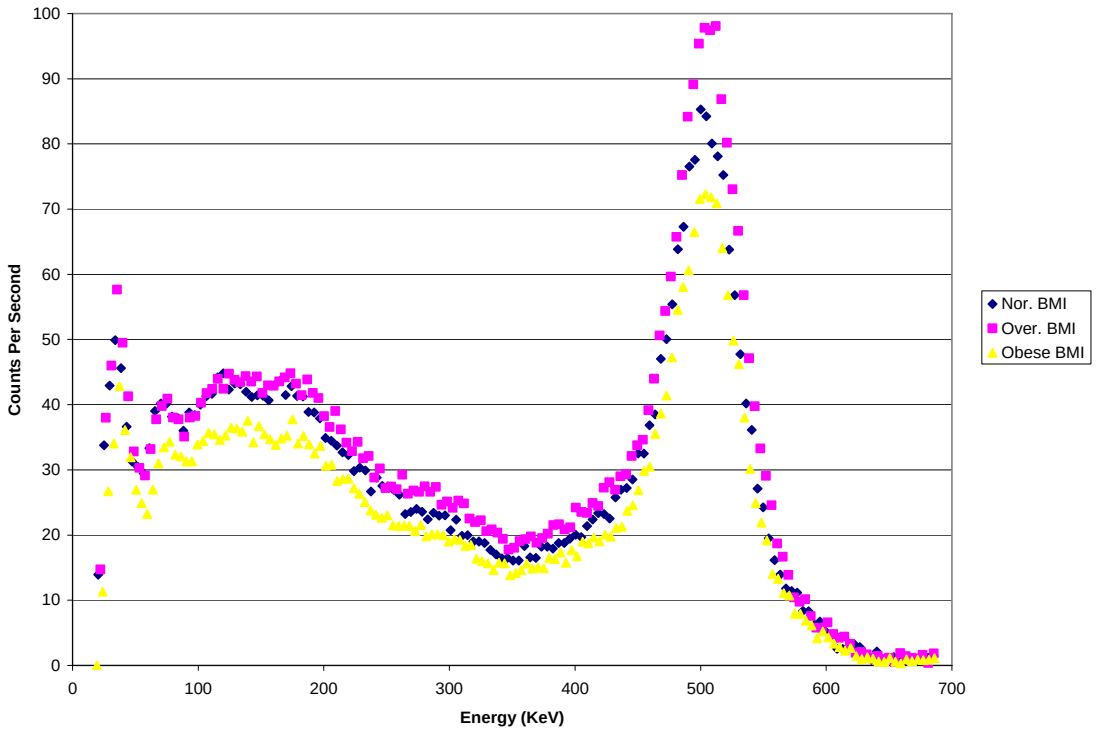

Figure 14. Three Outer Corridor Patient Spectra.

Figure 15 below shows the spectra emitted from the same three patients measured after passing through the unleaded wall in the inner corridor. In Figures 14 and 15, the spectra for the fourth patient measured in each of the three BMI categories (the last patient measured for Normal Weight, and the next to the last patient measured for both Overweight and Obese) are shown. (All 28 patient spectra measurements, and the background spectra measurements that were subtracted from the patient spectra measurements, are shown in the appendix.)

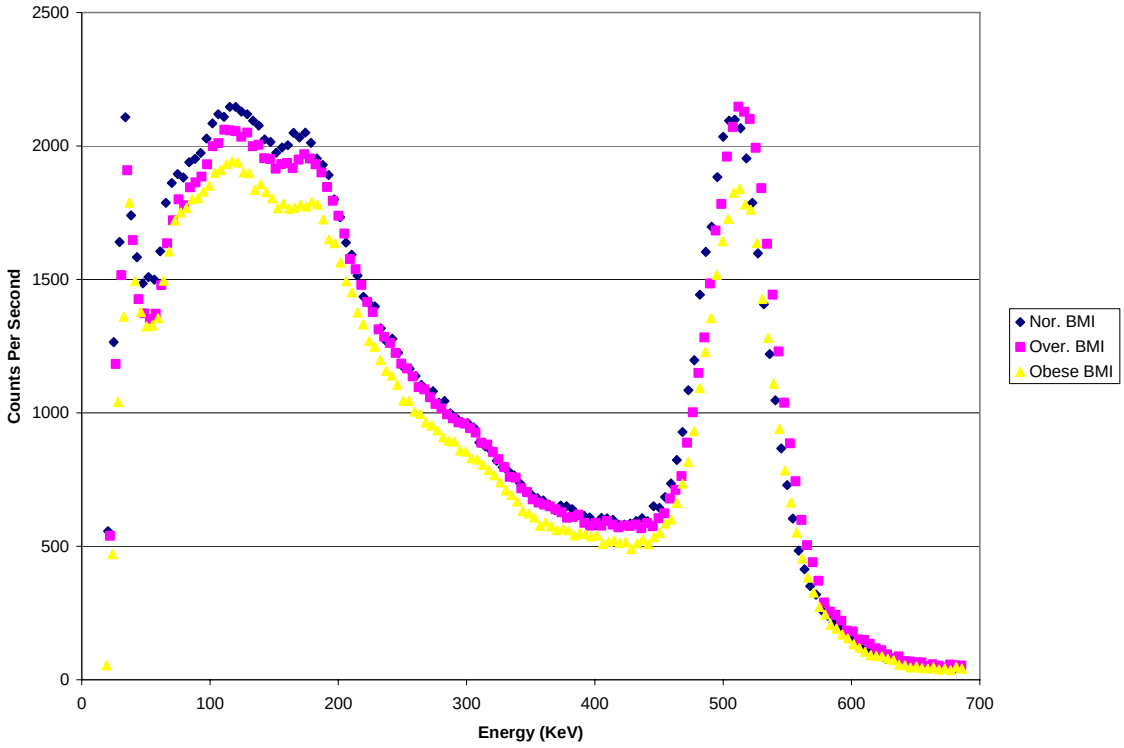

Figure 15. Three Inner Corridor Patient Spectra.

Patient Transmission Factors (Ratios)

The total corrected counts per second for all 28 patient spectra measurements are shown in Table 2 below. The transmission factors for 15.9 mm (5/8 inch)-thick lead shielding (B_{lead}) for each patient were calculated using equation 1. The transmission factors for all 14 patients measured at points 30.5 cm (1 foot) from the inner and outer corridor walls are given in Table 2. Average values are also given in Table 2. The average values of the ratios are important for the statistical analyses of the measurements.

Table 2

Corrected Counts Per Second and Ratios for All Patient Spectra Measurements

Patient	Total Corrected Counts Per Second, No Lead Shielding (N_o)	Total Corrected Counts Per Second, 15.9 mm Lead Shielding (N)	Transmission Factors (Ratios) At 30.5 cm (1 Foot) From Walls (B{lead})	
1	157585.3	4220.2	0.0268	
2	158125.3	4484.4	0.0284	
3	163810.9	4217.6	0.0257	
4	159889.2	4400.3	0.0275	
5	164455.8	4780.7	0.0291	
6	157907.7	3609.2	0.0229	
7	177616.5	3930.0	0.0221	
8	161122.6	4774.0	0.0296	
9	166368.0	4166.7	0.0250	
10	164310.0	5108.1	0.0311	
11	145621.7	3686.6	0.0253	
12	162019.3	4981.0	0.0307	
13	150573.0	4711.1	0.0313	
14	161890.8	4273.6	0.0264	
	160806.9	4381.7	0.0273	Average
	Average Total Counts Per Second			Ratio

Effective Body Absorption Factor and Spectrum Plot of Point Source of ^{18}F

Figure 16 below shows the spectrum emitted from a point source of ^{18}F FDG measured after penetrating through the unleaded wall. (Another point source spectrum measurement, and the background spectrum measurement that was subtracted from the point source spectra measurements, are shown in the appendix.)

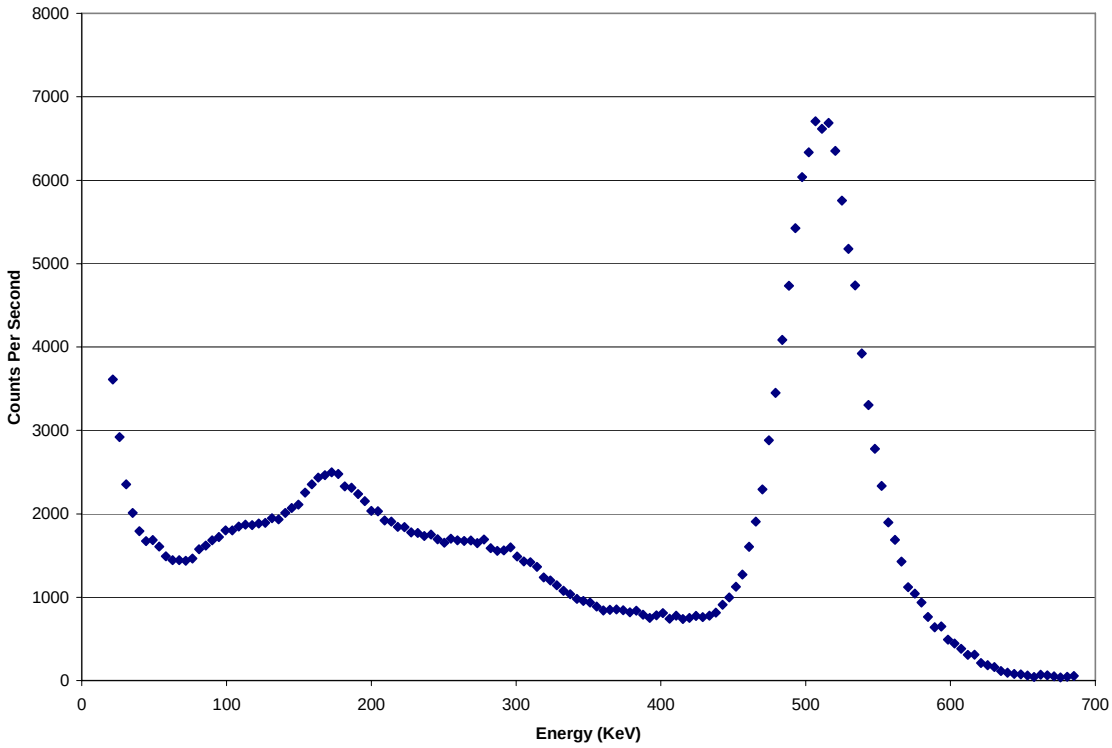

Figure 16. Point Source of ^{18}F Measured in Air.

The total corrected counts per second for measurements of the spectra emitted from a point source are shown in Table 3 below.

Table 3

Total Corrected Counts Per Second for Point Source Measurements

Point Source Measurement	Total Corrected Counts Per Second, No Lead Shielding (N_o)	
1	256777.4	
2	256914.4	
	256845.9	Average Total Counts Per Second

The effective body absorption factor was obtained by first dividing the average total corrected patient counts per second given in Table 2 (160806.9) by the average total point source corrected counts per second (256845.9) given in Table 3 to obtain the average amount of radiation emitted from the bodies of the patients (B_e):

$$B_e = \frac{160806.9}{256845.9} = 0.626.$$

The measured effective body absorption factor (B_a) is given by[1,15]:

$$B_a = 1 - 0.626 = 0.374. \qquad (5)$$

Patient and Phantom Spectra Plots

Figure 17 below shows the spectrum measured after penetrating through the leaded wall from ^{18}F mixed with the water inside the water-filled phantom that simulates adult patients, along with the three patient spectra shown in Figure 14 for comparison.

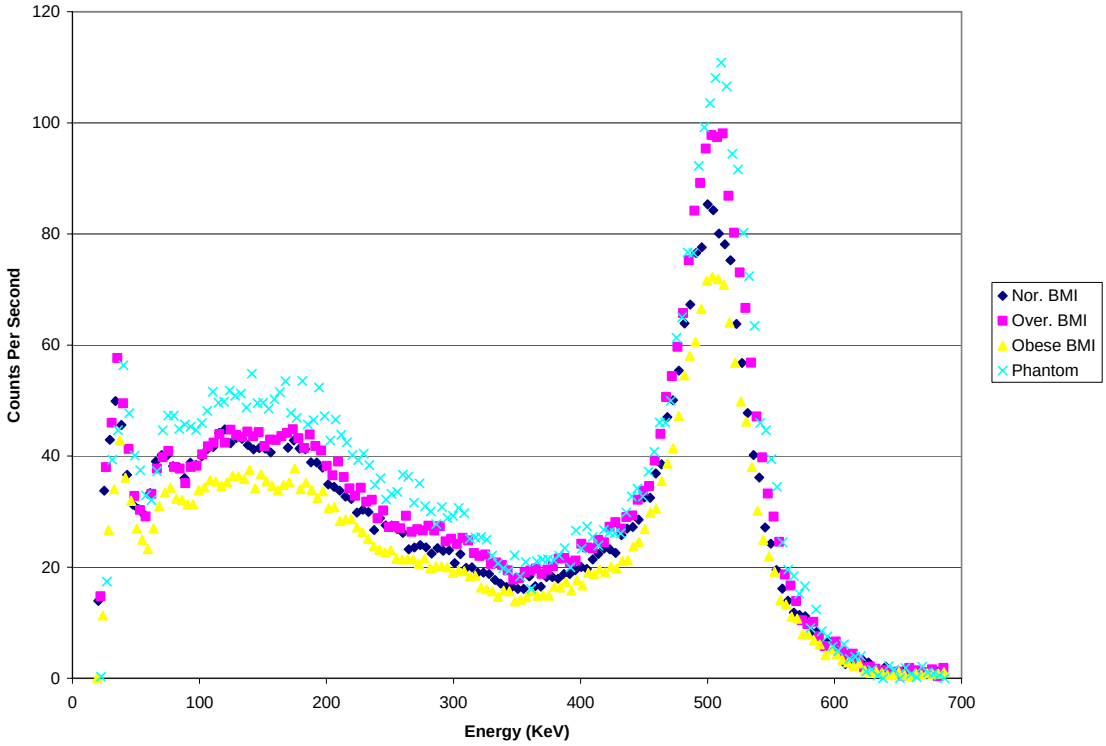

Figure 17. Leaded Wall Patient and Phantom Spectra.

Figure 18 below shows the spectrum emitted from the phantom measured after penetrating through the unleaded wall, along with the three patient spectra shown in Figure 15 for comparison. (Additional phantom spectra measurements, and the background spectrum measurement that was subtracted from the May 7th, 2010 phantom spectra measurements, are shown in the appendix.)

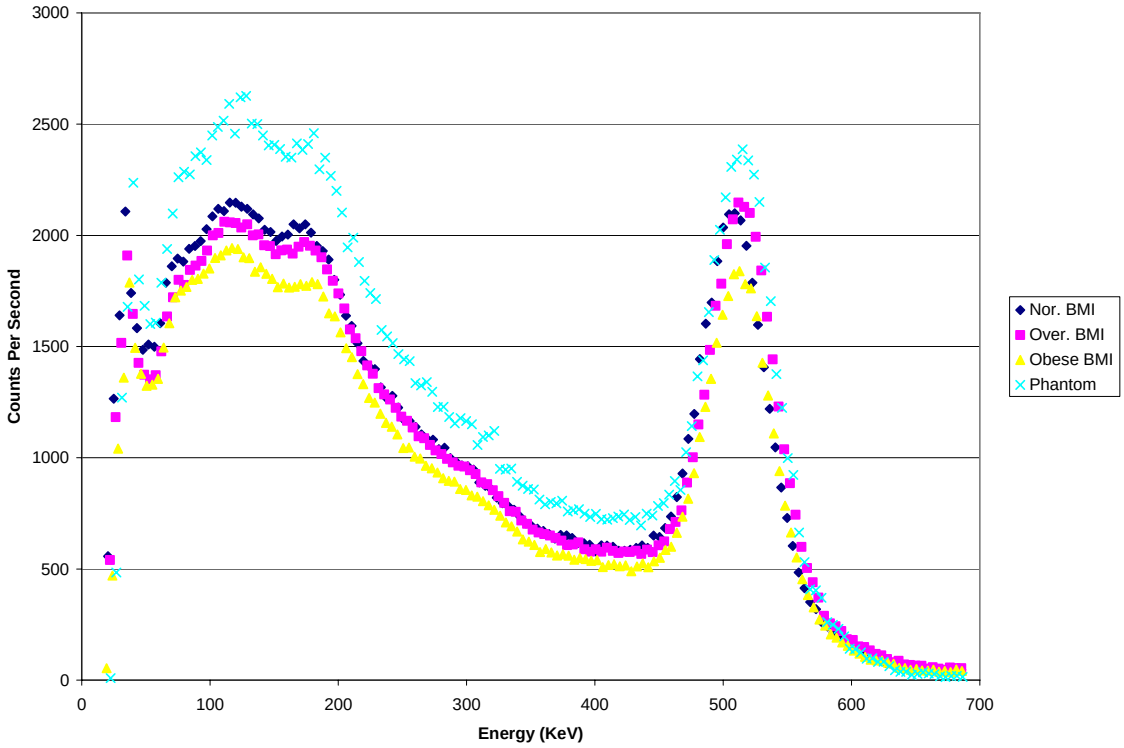

Figure 18. Unleaded Wall Patient and Phantom Spectra.

Phantom Transmission Factors (Ratios)

The transmission factors (ratios) for three sets of corresponding leaded and unleaded wall phantom spectra measurements were calculated using equation 1, and the factors for the phantom measured at points 30.5 cm (1 foot) from the outer and inner corridor walls are given below in Table 4.

Table 4

Phantom Transmission Factors Measured for 15.9 mm-Thick Lead Shielding

Phantom Spectra Measurement	Transmission Factors (Ratios) At 30.5 cm (1 Foot) From Walls (B{lead})	
1	0.0298	
2	0.0277	
3	0.0257	
	0.0277	Average Ratio

Effective Phantom Absorption Factor

The total corrected counts per second for the July 7th, 2010 measurements of the spectra emitted from the phantom are shown in Table 5 below.

Table 5

Total Corrected Counts Per Second for July 7th Phantom Measurements

Phantom Spectra Measurement	Total Corrected Counts Per Second, No Lead Shielding (N_o)	
1	193485.5	
2	188409.1	
	190947.3	Average Total Counts Per Second

The effective phantom absorption factor was obtained by dividing the average total phantom corrected counts per second given in Table 5 (190947.3) by the average total point

source corrected counts per second (256845.9) given in Table 3 to obtain the average amount of radiation emitted from the phantom (Ph_e):

$$Ph_e = \frac{190947.3}{256845.9} = 0.743.$$

The measured effective phantom absorption factor *(Ph_a)* is thus[1,15]:

$$Ph_a = 1 - 0.743 = 0.257. \qquad (6)$$

Angled Phantom Measurement

The patient measurements in the inner corridor were performed 43.2 cm (17 inches) to the left of a line perpendicular to the line connecting the center of the chair in the preparation room and the point used for the outer corridor measurements. In addition, the sodium iodide detector was pointed perpendicular to the inner corridor wall. Thus the radiation struck the sodium iodide detector at an oblique angle after penetrating through the unleaded inner corridor wall. The sodium iodide detector was pointed perpendicular to the inner corridor wall while patient measurements were taken for reproducibility. An investigation was made to determine if the counts per second detected would increase significantly if the detector in the inner corridor were pointed directly at the patients. A phantom measurement was made with the detector moved five inches parallel to the inner corridor wall and angled so that it was pointing directly at the center of the phantom. The total counts per second for this phantom measurement was 196653.5, which is 3.0% greater than the average total counts per second for the other two July 7th, 2010 inner corridor phantom measurements given in Table 5 (190947.3). Thus performing the inner

corridor patient measurements with the sodium iodide detector pointed directly at the patients while measurements were being taken would not have significantly increased the measured counts per second compared to taking the inner corridor patient measurements with the detector pointed perpendicular to the inner corridor wall.

Ionization Chamber Survey Meter Transmission Factors (Ratios)

The transmission factors (ratios) for all 14 patients, as measured by the ionization chamber survey meter at points 30.5 cm (1 foot) from the inner and outer corridor walls, are given below in Table 6. The corresponding patient spectrum transmission factors are included in Table 6 for comparison.

Table 6

Patient Spectra and Survey Meter Transmission Factors

	Transmission Factors (Ratios) At 30.5 cm (1 Foot) From Walls (B{lead})		
Patient	Spectra	Meter	
1	0.0268	0.0442	
2	0.0284	0.0426	
3	0.0257	0.0434	
4	0.0275	0.0481	
5	0.0291	0.0468	
6	0.0229	0.0451	
7	0.0221	0.0407	
8	0.0296	0.0469	
9	0.0250	0.0398	
10	0.0311	0.0480	
11	0.0253	0.0400	
12	0.0307	0.0529	
13	0.0313	0.0564	
14	0.0264	0.0445	
	0.0273	0.0457	Average Ratios

Modified Survey Meter Transmission Factors (Ratios)

The average survey meter ratio (0.0457) is 67.4% greater than the average spectra ratio (0.0273), which is a rather large discrepancy. The sodium iodide detector is shielded on its back and sides with lead. The survey meter does not have any lead shielding, so it detects radiation entering the ionization chamber inside the meter from its front, back, and sides[22]. In order to determine if radiation entering the meter from its sides was significantly affecting the survey meter ratios, lead sheets were used to wrap the sides of the survey meter. Ratios were measured and calculated with the meter un-

shielded, and with the sides of the meter shielded. The results for two patients are shown below in Table 7.

Table 7

Survey Meter Transmission Factors (Ratios) With and Without Lead Shielding

	Transmission Factors (Ratios) At 30.5 cm (1 Foot) From Walls (B{lead})		
Patient	Meter Without Lead Shielding	Meter With Lead Shielding	Percentage of Meter Ratio Reduction
1	0.0465	0.0341	26.7
2	0.0368	0.0273	25.8
			26.2 Average Percentage of Meter Ratio Reduction

In order to correct the results given in Table 6, the survey meter ratios were reduced by the average percentage of meter ratio reduction given in Table 7 (26.2). This enables a more direct comparison between the spectra and survey meter ratios, since the sodium iodide detector is shielded from radiation entering the sides of the detector. The results are shown below in Table 8.

Table 8

Patient Spectra and Shielded Survey Meter Transmission Factors

Patient	Transmission Factors (Ratios) At 30.5 cm (1 Foot) From Walls (B{lead}) Spectra	Meter With Lead	
1	0.0268	0.0326	
2	0.0284	0.0314	
3	0.0257	0.0320	
4	0.0275	0.0355	
5	0.0291	0.0345	
6	0.0229	0.0333	
7	0.0221	0.0300	
8	0.0296	0.0346	
9	0.0250	0.0294	
10	0.0311	0.0354	
11	0.0253	0.0295	
12	0.0307	0.0391	
13	0.0313	0.0416	
14	0.0264	0.0329	
	0.0273	0.0337	Average Ratios

The average shielded survey meter ratio (0.0337) is 23.4% greater than the average spectra ratio (0.0273). This is much smaller than the discrepancy between the average unshielded survey meter ratio and the average spectra ratio (67.4%).

Survey meter inaccuracy. The medical physicists in the University of Alabama at Birmingham (UAB) Department of Radiology tested the ionization chamber survey meter used in this research project (a FLUKE® Biomedical Model 451P Pressurized µR Ion Chamber Survey Meter) simultaneously with other survey meters, and found that the

Model 451P survey meter exposure rate readings differed by a factor of two or three from the exposure rate readings of the other survey meters tested at diagnostic x-ray energies. The reason for this discrepancy is that the chamber inside the Model 451P survey meter is pressurized. The technical data sheet for the Model 451P survey meter indicates that the gas inside the ion chamber inside this meter is pressurized at 125 pounds per square inch[22]. The thick plastic surrounding the ion chamber inside the Model 451P survey meter which keeps the gas under pressure also attenuates lower-energy radiation. Thus the Model 451P survey meter detects lower energy radiation with significantly less efficiency that the other survey meters that were tested. Because of this detection efficiency problem at lower energies with the Model 451P survey meter, from this point forward only the spectra results are given.

Statistical Analysis of Patient BMI Category and Phantom Ratios

The spectra transmission factors (ratios) for 15.9 mm (5/8 inch)-thick lead shielding (B_{lead}) for each patient, which are given in Table 2, were sorted from lowest to highest BMI. The spectra ratios were then arranged according to BMI category so that a one-way ANOVA statistical test could be performed on the data. The phantom spectra ratios given in Table 4 were also included as a category. The BMI that corresponds to each spectra ratio is given for all 14 patients in Table 9 below.

Table 9

Patient and Phantom Spectra Transmission Factors Arranged by Categories

	Transmission Factors (Ratios) At 30.5 cm (1 Foot) From Walls (B{lead})			
	BMI Categories			
	Normal	Overweight	Obese	Phantom
Spectra	0.0311	0.0221	0.0284	0.0298
Ratios	0.0313	0.0296	0.0307	0.0277
	0.0264	0.0250	0.0229	0.0257
	0.0268	0.0291	0.0257	
		0.0275	0.0253	
	Average Patient Ratios		0.0273	0.0277 Average Phantom Ratios
Corresponding	19.9	25.8	30.6	Phantom
Sorted	21.5	27.5	34.1	Measurement
Patient	21.8	27.5	35.9	1
BMI	22.7	27.7	37.1	2
		28.9	41.8	3

A one-way ANOVA statistical test was performed on the ratios in the categories given in Table 9. The results are given below in Table 10 and Table 11.

Table 10

Statistical Summary of Patient BMI and Phantom Ratio Categories

SUMMARY Groups	Count	Sum	Average	Variance
Normal	4	0.116	0.0289	7.1E-06
Overweight	5	0.133	0.0267	9.7E-06
Obese	5	0.133	0.0266	9.1E-06
Phantom	3	0.083	0.0277	4.2E-06

Table 11

One-Way ANOVA Results for Patient BMI and Phantom Ratio Categories

ANOVA Source of Variation	SS	df	MS	F	P-value	F crit
Between Groups	1.5E-05	3	5.1E-06	0.631	0.608	3.41
Within Groups	1.0E-04	13	8.1E-06			
Total	1.2E-04	16				

Statistical Analysis of Patient Reclining Angle Category Ratios

The spectra ratios given in Table 2 were sorted from lowest to highest reclining angle of patients in the chair in the patient preparation room. The spectra ratios were then arranged according to patient reclining angle category so that a one-way ANOVA statistical test could be performed on the data. The patient reclining angle that corresponds to each spectra ratio is given for all 14 patients in Table 12 below.

Table 12

Spectra Ratios Arranged by Patient Reclining Angle Categories

	Transmission Factors (Ratios) At 30.5 cm (1 Foot) From Walls (B{lead})			
	Estimated Angles in Degrees of Patients Reclining in Uptake Room Chair			
	≤ 40	40 < Angle ≤ 45	> 45	
Spectra Ratios	0.0268	0.0221	0.0229	
	0.0291	0.0311	0.0296	
	0.0313	0.0253	0.0284	
	0.0264	0.0250	0.0275	
		0.0307	0.0257	
			0.0273	Average Ratios
Corresponding Sorted Patient Reclining Angles	30-35	40-45	45-50	
	35-40	40-45	45-50	
	40	40-45	50-55	
	40	45	50-55	
		45	55-60	

A one-way ANOVA statistical test was performed on the ratios in the categories given in Table 12. The results are given below in Table 13 and Table 14.

Table 13

Statistical Summary of Patient Reclining Angle Ratio Categories

SUMMARY Groups	Count	Sum	Average	Variance
≤ 40	4	0.114	0.0284	5.2E-06
40 < Angle ≤ 45	5	0.134	0.0268	1.5E-05
> 45	5	0.134	0.0268	6.8E-06

Table 14

One-Way ANOVA Results for Patient Reclining Angle Ratio Categories

ANOVA Source of Variation	SS	df	MS	F	P-value	F crit
Between Groups	7.0E-06	2	3.5E-06	0.372	0.697	3.98
Within Groups	1.0E-04	11	9.5E-06			
Total	1.1E-04	13				

Calculating New Broad-Beam Transmission Factors

Determination of Transmission Factor (B_{lead}) for 15.9-mm Thick Lead

Estimates of the percentages of the patients of the TKC PET/CT Center that fall into the three BMI categories (Normal Weight, Overweight, and Obese) were calculated by the following methodology. Records of the 75 last patients of the day of the TKC PET/CT Center were obtained for the time period August 23, 2010—December 8, 2010. The height, weight, and date of measuring the height and weight, of each of the 75 patients, which are routinely recorded for all patients of the TKC PET/CT Center, were obtained. No other patient identifiers were obtained. The height, weight, and dates were entered into an Excel spreadsheet for all 75 patients. The BMI values were then calculated for all 75 patients using an online program provided by the National Institutes of Health[23], and checked with another online program provided by the Centers for Disease Control and Prevention[24]. The BMI values were then sorted using a program in Excel. The following percentages of the 75 patients that fall into each of the three BMI categories were then determined:

Normal Weight, $25 \div 75 = 33.3$ %; (7)

Overweight, $28 \div 75 = 37.3$ %; and (8)

Obese, $22 \div 75 = 29.3$ %. (9)

BMI category percentages of measured patients. The percentages of the 14 measured patients given in Table 9 that fall into each of the three BMI categories are as follows:

Normal Weight, $4 \div 14 = 28.6$ %; (10)

Overweight, $5 \div 14 = 35.7$ %; and (11)

Obese, $5 \div 14 = 35.7$ %. (12)

According to Table 9 and Table 10, the average ratio for each of the three patient BMI categories, and the overall average patient ratio are as follows:

$Ratio_{normal\ weight} = 0.0289$; (13)

$Ratio_{overweight} = 0.0267$; (14)

$Ratio_{obese} = 0.0266$; and (15)

$Ratio_{overall\ average} = 0.0273$. (16)

When equation 7 is compared to equation 10 (33.3 % vs. 28.6 %), equation 8 is compared to equation 11 (37.3 % vs. 35.7 %), and equation 9 is compared to equation 12 (29.3 % vs. 35.7 %), it is apparent that the percentages of the 75 last patients of the day at the TKC PET/CT Center in the three BMI categories are similar to the percentages of the 14 measured patients given in Table 9. Also, when equations 13, 14, and 15 are compared to

equation 16 (0.0289, 0.0267, and 0.0266 vs. 0.0273), it is apparent that the average ratios in each of the three patient BMI categories are similar to the overall average patient ratio. Since the percentages and ratios are so similar, the overall average transmission factor (ratio) of 0.0273 was used to calculate the new broad-beam lead transmission factors for patient spectra measurements at 511 keV.

New Broad-Beam Transmission Factors for Different Thicknesses of Lead

The value of the effective linear attenuation coefficient (μ_{lead}) was calculated with equation 2. Equation 2 gives a value of μ_{lead} = 0.226/mm for the patient spectra measurements. The value of the effective linear attenuation coefficient (μ_{lead}) was multiplied by different thicknesses of lead to obtain new broad-beam transmission factors for different thicknesses of lead at 511 keV using equation 3. These new broad-beam transmission factors are given in Table 15 below. This is provided as an estimate assuming that the effects for smaller thicknesses of lead are not different. The corresponding broad-beam transmission factor values given by AAPM Task Group 108 for different thicknesses of lead at 511 keV are included in Table 15 for comparison[1]. The new broad-beam transmission factors given in Table 15 should be used with caution, since they are based on measurements of radiation penetrating through only one thickness of lead (15.9 mm or 5/8 inches).

Table 15

New Broad-Beam Lead Transmission Factors at 511 keV

Thickness (mm lead)	Calculated Lead Transmission Factor	AAPM Task Group 108 Lead Transmission Factor
0	1.000	1.000
1	0.798	0.891
2	0.636	0.787
3	0.508	0.690
4	0.405	0.602
5	0.323	0.523
6	0.258	0.452
7	0.206	0.390
8	0.164	0.336
9	0.131	0.289
10	0.104	0.248
11	0.083	
12	0.066	0.183
13	0.053	
14	0.042	0.135
15	0.034	
16	0.027	0.099
17	0.021	
18	0.017	0.073
19	0.014	
20	0.011	0.054
21	0.009	
22	0.007	
23	0.006	
24	0.004	
25	0.004	0.025
26	0.003	

CHAPTER 5

DISCUSSION

Measurements of the spectra of radiation emitted from adult patients administered ^{18}F FDG of different BMI were performed in a clinical setting at The Kirklin Clinic PET/CT Center to determine experimentally if current shielding designs for PET or PET/CT imaging facilities using lead shielding result in safety margins that are higher than originally calculated to adequately protect public health. Measurements were also made of ^{18}F measured after being mixed with the water inside an elliptical water-filled phantom that simulates adult patients, and of a point source of ^{18}F.

Inner and Outer Corridor Patient Spectra Comparison

When Figure 14 (outer corridor) is compared to Figure 15 (inner corridor), it is clear that spectra emitted from patients measured after penetrating through the unleaded wall in the inner corridor showed more counts per second having energies significantly lower than the 511-keV peak, when compared to the spectra emitted from the same patients measured after penetrating through the wall in the outer corridor, as expected. It is also seen that much of the lower-energy scatter radiation in Figure 15 is not seen in Figure 14. This was expected, because the 15.9 mm (5/8 inch)-thick lead shielding in the outer corridor wall should absorb a larger fraction of the lower-energy scatter radiation. A comparison of Figure 14 and Figure 15 also shows that the spectra emitted from pa-

tients did not appear to be significantly altered when the BMI changed. One reason for the lack of significant alteration of the spectra is because the 511-keV annihilation radiation photons resulting from the decay of ^{18}F are not easily attenuated by human tissue.

Point Source Spectra Compared to Patient Spectra

As can be seen in Figure 16, a point source measured in air has significantly more counts per second at the 511-keV peak than in Figure 15, which is expected, since patients absorb a large percentage of the radiation emitted by the ^{18}F FDG. Figure 16 shows most of the counts close to the 511-keV peak, with little scatter. Figure 15 shows a significant scatter distribution, with many counts having energies significantly lower than 511 keV, which was expected.

Effective Body Absorption Factor

An effective body absorption factor of 0.37 was measured. This is in good agreement with the effective body absorption factor of 0.36 recommended by AAPM Task Group 108[1,15].

Phantom Spectra Compared to Patient Spectra

The phantom spectrum measured through the leaded wall in Figure 17 appears to be very similar to the patient spectra in Figure 17. The phantom spectrum taken through the unleaded wall in Figure 18 appears to be very similar to the patient spectra in Figure 18.

Effective Phantom Absorption Factor

An effective phantom absorption factor of 0.26 was measured. This is significantly less than the effective body absorption factor of 0.37 that was measured. This result is not surprising, because the phantom is smaller than the human body, so there is less mass in the phantom to absorb the annihilation radiation.

Modified Ionization Chamber Survey Meter Transmission Factors

The modified ionization chamber survey meter patient transmission factors (ratios) were in reasonably good agreement with the patient spectra transmission factors. The survey meter measurements were used as a second means to verify the results. The pressurized chamber inside the survey meter is very sensitive for detecting radiation, but has low detection efficiency at lower energies. An ionization chamber survey meter with an unpressurized chamber may have higher detection efficiency at lower energies, but may not be adequately sensitive for detecting radiation, particularly the low radiation exposure levels that penetrated through the leaded wall in the outer corridor. The needle of a Geiger counter may fluctuate too much to be used when measuring the low radiation exposure levels in the outer corridor. The modified survey meter ratios were not used further because of the low detection efficiency at lower energies for the survey meter used in this research project.

Statistical Analysis of Patient BMI and Phantom Ratios

The average transmission factor (ratio) values given for each of the three patient BMI categories (Normal Weight, Overweight, and Obese) given in Table 10 (0.0289, 0.0267, and 0.0266) appear to be very close to each other, and to the overall patient ratio

given in Table 6 (0.0273). The average phantom ratio given in Table 9 (0.0277) also appears to be very close to the overall patient ratio. A one-way ANOVA statistical test was performed on the ratios arranged according to patient BMI category, with the phantom ratios also included as a category. The one-way ANOVA gave a p-value of 0.608, which is much higher than a p-value of 0.05. Thus there are no statistically significant differences between the average patient BMI category and phantom ratios.

Statistical Analysis of Patient Reclining Angle Ratios

The average transmission factor (ratio) values given for each of the three angles of patients reclining in the chair in the patient preparation room categories (≤ 40 degrees, 40 degrees < angle ≤ 45 degrees, and > 45 degrees) given in Table 13 (0.0284, 0.0268, and 0.0268) appear to be very close to each other, and to the overall patient ratio given in Table 6 (0.0273). A one-way ANOVA statistical test was performed on the ratios arranged according to patient reclining angle category. The one-way ANOVA gave a p-value of 0.697, which is much higher than a p-value of 0.05. Thus there are no statistically significant differences between the average patient reclining angle category ratios.

Generating a New Paradigm for Shielding of PET/CT Medical Centers

For a particular thickness of lead shielding (other than zero), the new broad-beam transmission factors given in Table 15 are significantly less than the corresponding broad-beam transmission factors in lead at 511 keV given by AAPM Task Group 108[1]. The outer corridor lead thickness of 15.9 mm at The Kirklin Clinic PET/CT Center is constructed to a transmission factor of one TVL (0.1) according to AAPM Task Group

108[1], which is a not uncommon amount of shielding for PET/CT medical centers[15]. Elschot, de Wit, and deJong found that a TVL of shielding for a PET or PET/CT facility is 13.3 mm of lead[15]. Using the value of the effective linear attenuation coefficient μ_{lead} = 0.226/mm that was measured in this work, a TVL of shielding for a PET or PET/CT facility has been experimentally determined to be 10.2 mm of lead. Thus current shielding designs for PET or PET/CT imaging facilities using lead shielding result in safety margins that are higher than generally assumed to adequately protect public health.

Other PET/CT Medical Center Lead Shielding Thicknesses

The new broad-beam transmission factors at 511 keV should be used with caution, because they are based on spectra transmission factor measurements made after radiation penetrated through a wall that contains only one thickness of lead shielding (15.9 mm or 5/8 inches). The results may not be applicable to other PET/CT centers that use different thicknesses of lead shielding.

CHAPTER 6

SUMMARY AND CONCLUSIONS

Increased Effective Attenuation Coefficient of Lead Shielding

The spectra of radiation emitted from adult patients administered ^{18}F FDG of different BMI were measured in this study in order to determine how scatter and absorption of radiation by the human body affect the transmission factors of radiation measured after penetrating through the 15.9 mm (5/8 inch)-thick lead in the outer corridor wall of The Kirklin Clinic PET/CT Center. The spectra emitted from patients showed that many of the energies were significantly lower than the 511-keV peak compared to the spectra emitted by a point source of ^{18}F. The measurements also showed that much of the lower-energy scatter radiation measured after penetrating through the unleaded inner corridor wall in The Kirklin Clinic PET/CT Center was absorbed when penetrating through the leaded wall, as was expected. The scatter of the annihilation radiation and the subsequent absorption of the lower-energy scattered radiation by the lead shielding resulted in an increase in the effective attenuation coefficient for lead. Because of the increased effective attenuation coefficient for lead, current shielding designs for PET or PET/CT imaging facilities using lead shielding result in safety margins that are higher than originally calculated to adequately protect public health.

Accuracy of Patient Spectra Measurements

Two checks were performed of the reliability of the spectra measurements taken with the sodium iodide detector. The measured effective body absorption factor of 0.37 is in excellent agreement with the effective body absorption factor of 0.36 recommended by AAPM Task Group 108[1]. Also, the modified ionization chamber survey meter patient ratios were in reasonably good agreement with the patient spectra ratios. Thus the measured spectra ratios appear to be reasonably accurate.

Patient BMI, Patient Uptake Chair Reclining Angle, and Phantom

By statistically analyzing the measurements results it was determined that neither differences in patient BMI nor differences in angles of patients reclining in the chair in the patient preparation room significantly affected the measured spectra ratios. It was also determined that the measured phantom spectra ratios are not significantly different from the measured patient spectra ratios. Thus the transmission factors for lead shielding in PET/CT imaging facilities can be accurately determined by measuring the spectra emitted from ^{18}F mixed with the water inside an elliptical water-filled phantom that simulates adult patients, instead of measuring the spectra emitted from patients.

New Broad-Beam Transmission Factors for Lead Shielding at 511 keV

The effective linear attenuation coefficient μ_{lead} = 0.226/mm that was measured in this study was used to generate a table of new broad-beam transmission factors for different thicknesses of lead at 511 keV. The following three examples show how the new broad-beam transmission factors can be used to demonstrate that current shielding de-

signs for PET or PET/CT imaging facilities using lead shielding result in safety margins that are higher than originally calculated to adequately protect public health, and to generate more accurate radiation exposure estimates for members of the public located adjacent to PET or PET/CT medical facilities that are shielded with lead. One of the examples shows how the new broad-beam transmission factors can be used to determine if existing lead shielding meets stricter NRC regulatory requirements.

Example Calculations Using New Broad-Beam Lead Transmission Factors

Equation 4 can be used can be used to calculate the maximum transmission factors necessary to meet current regulatory requirements for uncontrolled (B_U) areas located adjacent to a patient preparation room for the uptake of ^{18}F FDG[1]. For the following three examples, it is assumed that in equation 4:

$d^2 = 25$ m^2,

$T = 1$,

$N_W = 40$ patients per week,

$A_0 = 555$ MBq,

$t_U(h) = 1$ h, and for an uptake time of 1 h,

$R_{tU} = 0.83$[1].

Example 1

Using the parameters given above, how much lead shielding is required for an uncontrolled area? Using the above parameters in equation 4,

$B_U = 218 \times 25\ m^2 \div [1 \times 40$ patients per week $\times$ 555 MBq $\times$ 1 h $\times$ 0.83] = 0.296.

According to AAPM Task Group 108, 9 mm of lead shielding is required[1]. Using the new broad-beam lead transmission factors, according to Table 15, 6 mm of lead shielding is required.

Example 2

Using the parameters given above in equation 4, the weekly dose without lead shielding is:

$$\frac{\text{20 microSieverts (μSv)}}{0.296} = 67.6\ \mu Sv^{[1]}.$$

If the radiation is transmitted through 16 mm of lead shielding, which is about equal to the lead shielding thickness in the outer corridor of the TKC PET/CT Center (15.9 mm), what is the weekly dose? According to AAPM Task Group 108, $B_{lead} = 0.099$, the weekly dose is:

$$67.6\ \mu Sv \times 0.099 = 6.7\ \mu Sv^{[1]}.$$

Using the new broad-beam lead transmission factors, according to Table 15, $B_{lead} = 0.027$, the weekly dose is:

$$67.6\ \mu Sv \times 0.027 = 1.8\ \mu Sv.$$

Example 3

The NRC lowers the effective dose equivalent that members of the general public can receive in uncontrolled areas from no more than 1 mSv/year to no more than 0.25 mSv/year. This would reduce the weekly dose for uncontrolled areas from no more than 20 μSv to no more than 5 μSv[1]. Using the parameters given above in equation 4, if 16 mm of lead shielding is already in place in a PET/CT imaging facility, would additional lead shielding be required in order to meet the new NRC effective dose equivalent standards for members of the general public? According to AAPM Task Group 108 and Example 2, the weekly dose is 6.7 μSv, which is greater than 5 μSv, so additional lead shielding would be required in order to meet the new NRC effective dose equivalent standards for members of the general public[1]. According to Table 15 and Example 2, the weekly dose is 1.8 μSv, which is less than 5 μSv, so no additional lead shielding would be required in order to meet the new NRC effective dose equivalent standards for members of the general public.

Future Research

The new broad-beam transmission factors for different thicknesses of lead at 511 keV are based on spectra transmission factor measurements made after radiation penetrated through only one thickness of lead shielding (15.9 mm or 5/8 inches). Measurements of transmission factors should be made of radiation that penetrates through other thickness of lead shielding used in PET/CT medical centers (25.4 mm or 1 inch, 19.0 mm or ¾ inch, 12.7 mm or ½ inch, etc.) to determine if the new broad-beam transmission factors are valid for other thicknesses of lead shielding. One would expect less of an effect

at smaller thicknesses of lead. Also, broad-beam transmission factors at 511 keV should be measured for other shielding materials used in PET/CT medical centers, such as concrete and iron[1,15]. For future publication, more shielded survey meter readings may be taken. A better sodium iodide detector efficiency curve may be obtained by taking more measurements with different radioisotopes that were used in this study, and by repeating previous radioisotope measurements. Also, the patient spectra measurements could be converted to exposure values per hour using the energy dependent value of the mass energy absorption coefficient for air[25].

LIST OF REFERENCES

[1]Madsen, M., *et al.*, "AAPM Task Group 108: PET and PET/CT Shielding Requirements," Medical Physics: **33**, 4-15 (2006).

[2]Academy of Molecular Imaging (2008). *AMI Member PET Centers.* Retrieved February 13, 2011, from http://www.ami-imaging.org/index.php?option=com_content&task=view&id=91&Itemid=107.

[3]Centers for Disease Control and Prevention, Your Online Source for Credible Health Information, Healthy Weight-it's not a diet, it's a lifestyle (2009)! *About BMI for Adults.* Retrieved February 12, 2011, from http://www.cdc.gov/healthyweight/assessing/bmi/adult_bmi/index.html#Interpreted.

[4]RadiologyInfo™, The radiology information resource for patients (2009). *How does the procedure work?* Retrieved April 13, 2009, from http://www.radiologyinfo.org/en/info.cfm?PG=pet.

[5]Bushberg, J., *et al.*,*The Essential Physics of Medical Imaging, Second Edition* (Lippincott Williams & Wilkins, Philadelphia, PA, 2002, pp. 720-723).

[6]Bushberg, J., *et al.*,*The Essential Physics of Medical Imaging, Second Edition* (Lippincott Williams & Wilkins, Philadelphia, PA, 2002, pp. 45, 758).

[7]Bushberg, J., *et al.*,*The Essential Physics of Medical Imaging, Second Edition* (Lippincott Williams & Wilkins, Philadelphia, PA, 2002, pp. 34-40).

[8]Bushberg, J., *et al.*,*The Essential Physics of Medical Imaging, Second Edition* (Lippincott Williams & Wilkins, Philadelphia, PA, 2002, pp. 48).

[9]Erdman, M., King, S., and Miller, K., "Recent Experiences with Shielding a PET/CT Facility," Health Physics: **87**, Supplement 1, S37-S39, (2004).

[10]A. Bixler, G. Springer, and R. Lovas, "Practical aspects of radiation safety for using fluorine-18," J. Nucl. Med. Technol. **27**, 14–16 (1999).

[11] NCRP, *NCRP Report 49: Structural Shielding Design and Evaluation for Medical Use of X Rays and Gamma Rays of Energies up to 10 MeV* (National Council on Radiation Protection, Bethesda, MD, 1976).

[12] T. M. Lundberg, P. J. Gray, and M. L. Bartlett, "Measuring and minimizing the radia tion dose to nuclear medicine technologists," J. Nucl. Med. Technol. **30**, 25–30 (2002).

[13] N. A. Benatar, B. F. Cronin, and M. J. O'Doherty, "Radiation dose rates from patients undergoing PET: Implications for technologists and waiting areas," Eur. J. Nucl. Med. **27**, 583–589 (2000).

[14] B. W. Zeff and M. V. Yester, "Patient self-attenuation and technologist dose in positron emission tomography," Med. Phys. **32**, 861–865 (2005).

[15] M. Elschot, T. C. de Wit, and H. W. A. M. deJong, "The influence of self-absorption on PET and PET/CT shielding requirements," Medical Physics: **37** (6), 2999-3007 (2010).

[16] *Radiation Safety Procedures, PET Imaging Area* (The Kirklin Clinic, 2007).

[17] Radiation Safety Division Staff, *et al.*, *Radiation Safety Training Manual, 2002 Edition* (Radiation Safety Program, University of Alabama at Birmingham, 2002).

[18] Bushberg, J., *et al.*,*The Essential Physics of Medical Imaging, Second Edition* (Lippincott Williams & Wilkins, Philadelphia, PA, 2002, p. 647).

[19] Bushberg, J., *et al.*,*The Essential Physics of Medical Imaging, Second Edition* (Lippincott Williams & Wilkins, Philadelphia, PA, 2002, p. 628).

[20] Bushberg, J., *et al.*,*The Essential Physics of Medical Imaging, Second Edition* (Lippincott Williams & Wilkins, Philadelphia, PA, 2002).

[21] Procedure List, Psych 205 (2000). *One-Way ANOVA.* Retrieved February 19, 2011, from http://www.wellesley.edu/Psychology/Psych205/anova.html.

[22] FLUKE® Biomedical, 451B/451P Ion Chamber Survey Meter with Beta Slide/Pressurized µR Ion Chamber Survey Meter (2008). *Technical Data.* Retrieved February 20, 2011, from http://www.maquet-dynamed.com/inside_sales/literature/fluke/451p_and_b_datasheet.pdf.

[23]U.S. Department of Health & Human Services, National Heart Lung and Blood Institute, National Institutes of Health (2010). *Calculate Your Body Mass Index.* Retrieved December 20, 2010, from http://www.nhlbisupport.com/bmi/.

[24]Centers for Disease Control and Prevention, Your Online Source for Credible Health Information, Healthy Weight-it's not a diet, it's a lifestyle (2010)! *Adult BMI Calculator: English.* Retrieved December 20, 2010, from http://www.cdc.gov/healthyweight/assessing/bmi/adult_bmi/english_bmi_calculator/bmi_calculator.html.

[25]Beutel, J., Kundel, H., and Van Metter, R., *Handbook of Medical Imaging, Volume 1. Physics and Psychophysics* (SPIE—The International Society for Optical Engineering, Bellingham, WA, 2000, p. 38).

APPENDIX A

IRB APPROVAL FORM FOR RESEARCH PROJECT

THE UNIVERSITY OF ALABAMA AT BIRMINGHAM

Institutional Review Board for Human Use

Form 4: IRB Approval Form
Identification and Certification of Research
Projects Involving Human Subjects

UAB's Institutional Review Boards for Human Use (IRBs) have an approved Federalwide Assurance with the Office for Human Research Protections (OHRP). The Assurance number is FWA00005960 and it expires on September 29, 2013. The UAB IRBs are also in compliance with 21 CFR Parts 50 and 56.

Principal Investigator:	BRINKLEY, BRADLEY S.
Co-Investigator(s):	WHITE, SHARON L YESTER, MICHAEL V
Protocol Number:	**X091119018**
Protocol Title:	*Experimental Determination of Shielding Requirements for PET Medical Facilities*

The IRB reviewed and approved the above named project on 10-22-10. The review was conducted in accordance with UAB's Assurance of Compliance approved by the Department of Health and Human Services. This Project will be subject to Annual continuing review as provided in that Assurance.

This project received EXPEDITED review.

IRB Approval Date: 10-22-10

Date IRB Approval Issued: 10-22-10

HIPAA Waiver Approved?: Yes

Marilyn Doss

Marilyn Doss, M.A.
Vice Chair of the Institutional Review
Board for Human Use (IRB)

Investigators please note:

The IRB approved consent form used in the study must contain the IRB approval date and expiration date.

IRB approval is given for one year unless otherwise noted. For projects subject to annual review research activities may not continue past the one year anniversary of the IRB approval date.

Any modifications in the study methodology, protocol and/or consent form must be submitted for review and approval to the IRB prior to implementation.

Adverse Events and/or unanticipated risks to subjects or others at UAB or other participating institutions must be reported promptly to the IRB.

470 Administration Building
701 20th Street South
205.934.3789
Fax 205.934.1301
irb@uab.edu

The University of
Alabama at Birmingham
Mailing Address:
AB 470
1530 3RD AVE S
BIRMINGHAM AL 35294-0104

THE UNIVERSITY OF ALABAMA AT BIRMINGHAM

Institutional Review Board for Human Use

PI: BRINKLEY, BRADLEY S.
Protocol # X091119018

UAB IRB Approval of
Waiver of Informed Consent and/or Waiver of Patient Authorization

☐ **Approval of Waiver of Informed Consent to Participate in Research.** The IRB reviewed the proposed research and granted the request for waiver of informed consent to participate in research, based on the following findings:

1. The research involves no more than minimal risk to the subjects.
2. The research cannot practicably be carried out without the waiver.
3. The waiver will not adversely affect the rights and welfare of the subjects.
4. When appropriate, the subjects will be provided with additional pertinent information after participation.

Check one:
- ☐ **and** Waiver of Authorization (below)
- ☑ **or** Waiver of Authorization (below)
- ☐ Waiver of Authorization not applicable

☑ **Approval of Waiver of Patient Authorization to Use PHI in Research.** The IRB reviewed the proposed research and granted the request for waiver of patient authorization to use PHI in research, based on the following findings:

1. The use/disclosure of PHI involves no more than minimal risk to the privacy of individuals
   - i. There is an adequate plan to protect the identifiers from improper use and disclosure.
   - ii. There is an adequate plan to destroy the identifiers at the earliest opportunity consistent with conduct of the research, unless there is a health or research justification for retaining the identifiers or such retention that is otherwise required by law.
   - iii. There is an assurance that the PHI will not be reused or disclosed to any other person or entity, except as required by law, for authorized oversight of the research study, or for other research for which the use or disclosure of PHI would be permitted.
2. The research cannot practicably be conducted without the waiver or alteration.
3. The research cannot practicably be conducted without access to and use of the PHI.

—OR—

☐ **Full Review**

The IRB reviewed the proposed research at a **convened meeting** at which a majority of the IRB was present, including one member who is not affiliated with any entity conducting or sponsoring the research, and not related to any person who is affiliated with any of such entities. The waiver of authorization was approved by the majority of the IRB members present at the meeting.

Date of Meeting

Signature of Chair, Vice-Chair or Designee

Date

☑ **Expedited Review**

The IRB used an **expedited review procedure** because the research involves no more than minimal risk to the privacy of the individuals who are the subject of the PHI for which use or disclosure is being sought. The review and approval of the waiver of authorization were carried out by the Chair of the IRB, or by one of the Vice-Chairs of the IRB as designated by the Chair of the IRB.

10-22-10
Date of Expedited Review

Maureen Joss
Signature of Chair, Vice-Chair or Designee

Date 10-22-10

470 Administration Building
701 20th Street South
205.934.3789
Fax 205.934.1301
irb@uab.edu

The University of
Alabama at Birmingham
Mailing Address:
AB 470
1530 3RD AVE S
BIRMINGHAM AL 35294-0104

APPENDIX B

PATIENT, PHANTOM, BACKGROUND, AND POINT SOURCE SPECTRA

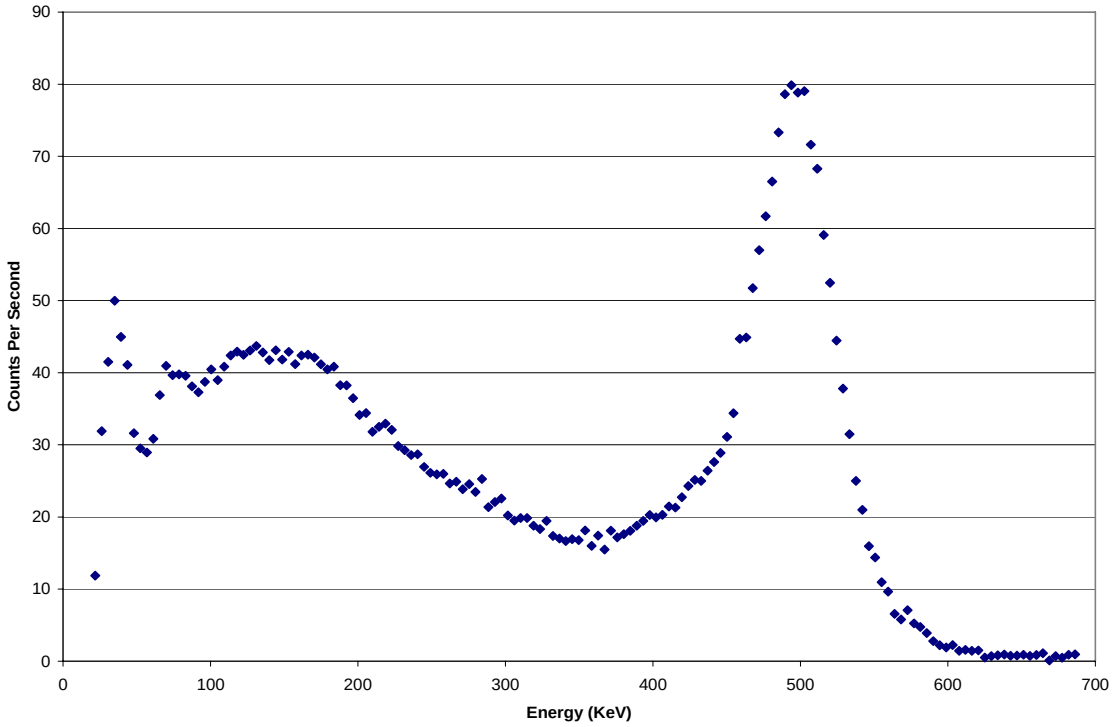

June 2, 2010 Outer Corridor Leaded Wall Patient Spectrum Measurement.

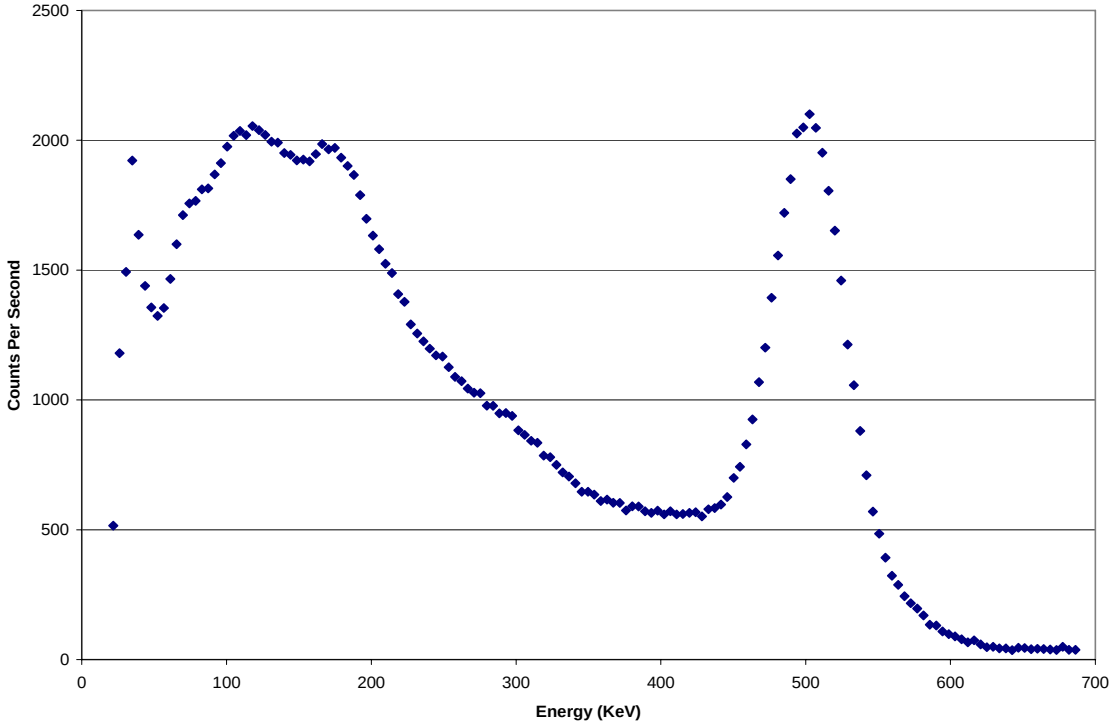

June 2, 2010 Inner Corridor Unleaded Wall Patient Spectrum Measurement.

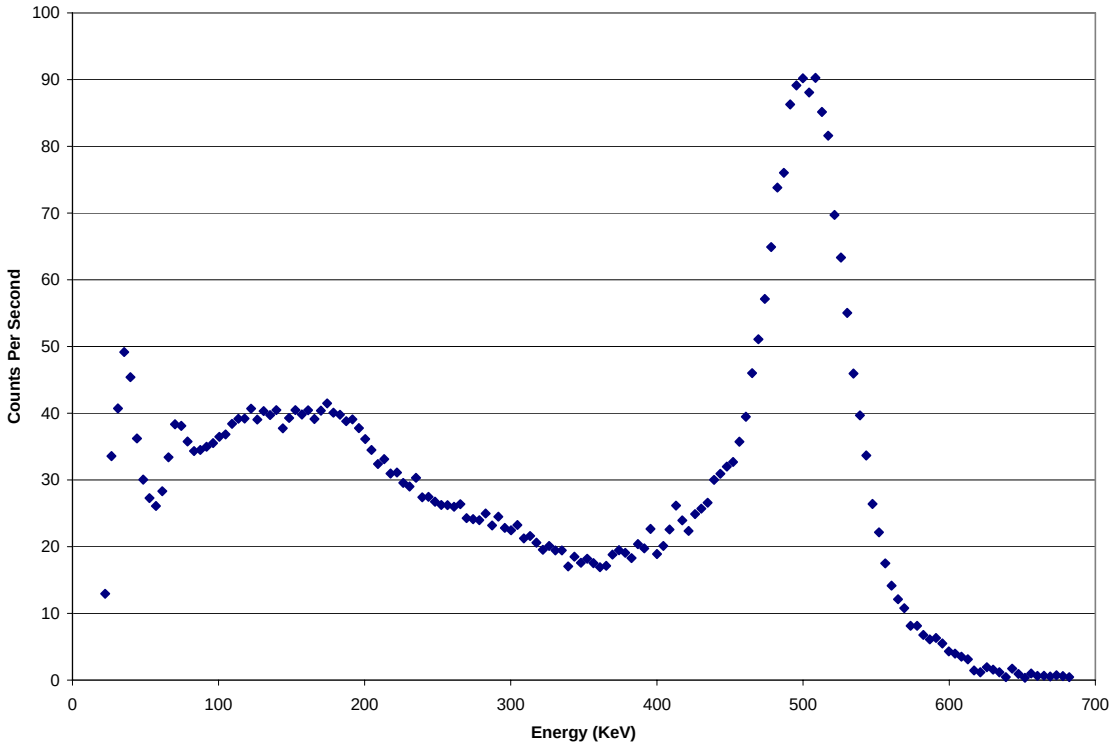

June 23, 2010 Outer Corridor Leaded Wall Patient Spectrum Measurement.

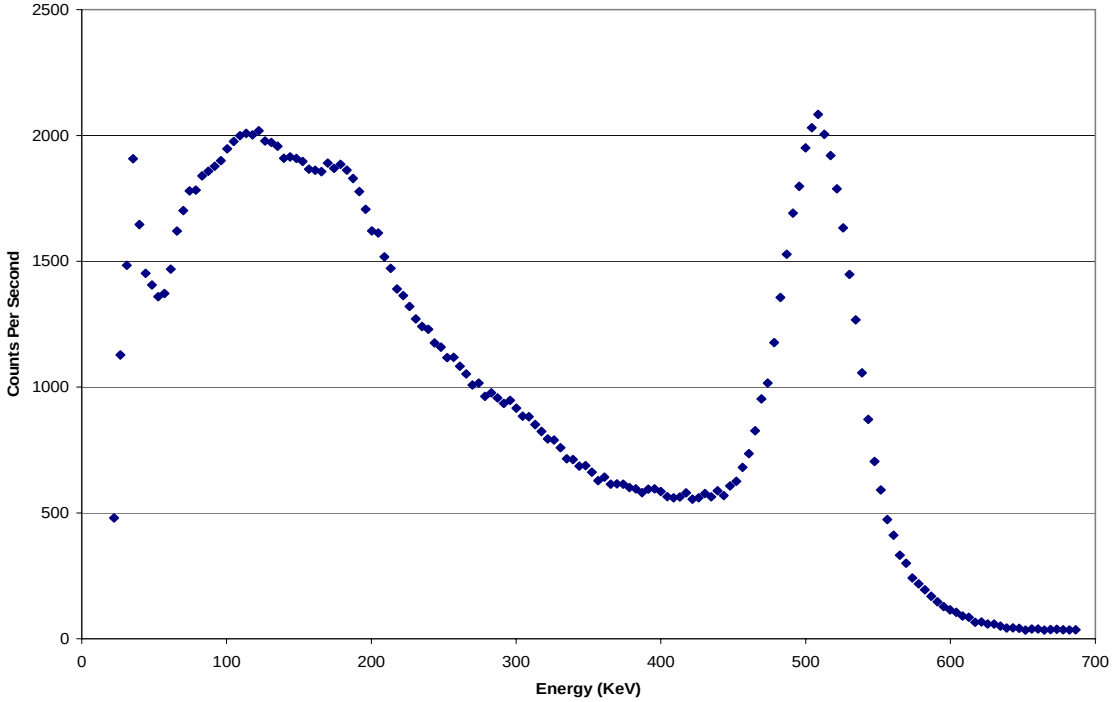

June 23, 2010 Inner Corridor Unleaded Wall Patient Spectrum Measurement.

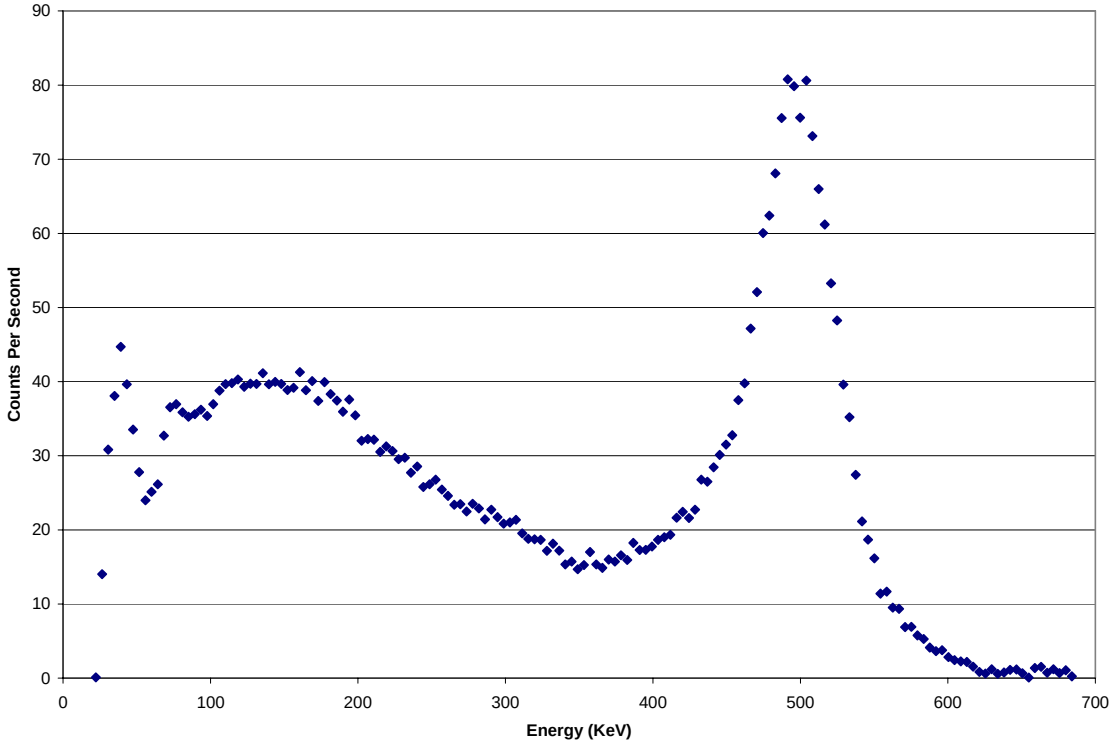

July 1, 2010 Outer Corridor Leaded Wall Patient Spectrum Measurement.

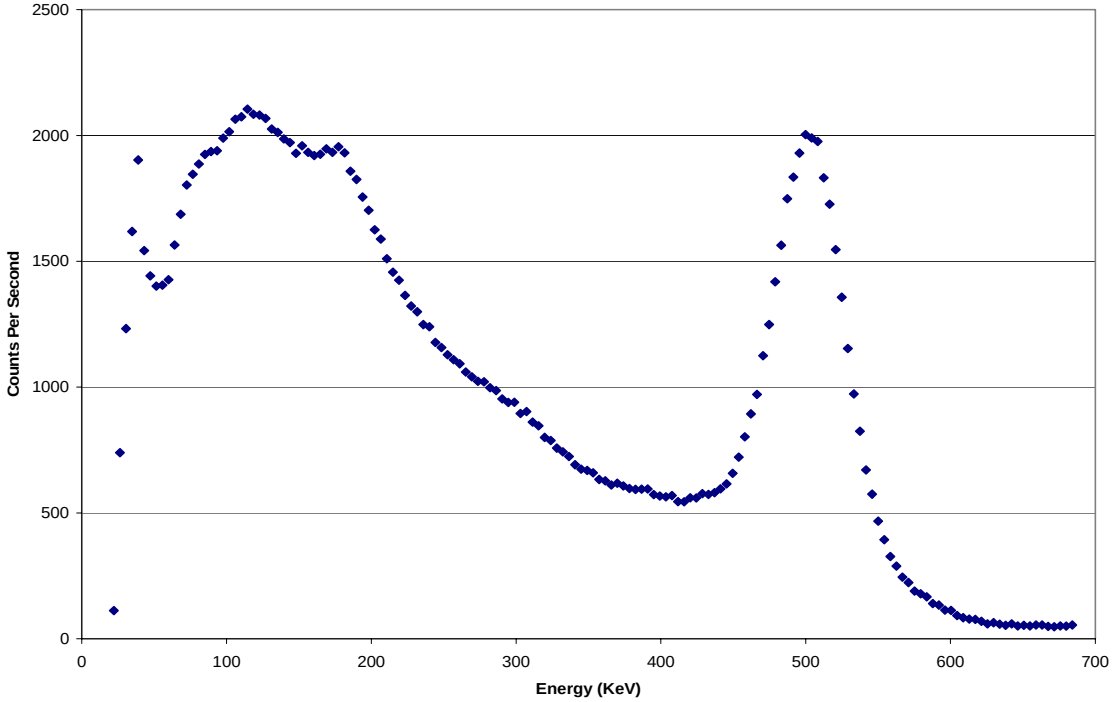

July 1, 2010 Inner Corridor Unleaded Wall Patient Spectrum Measurement.

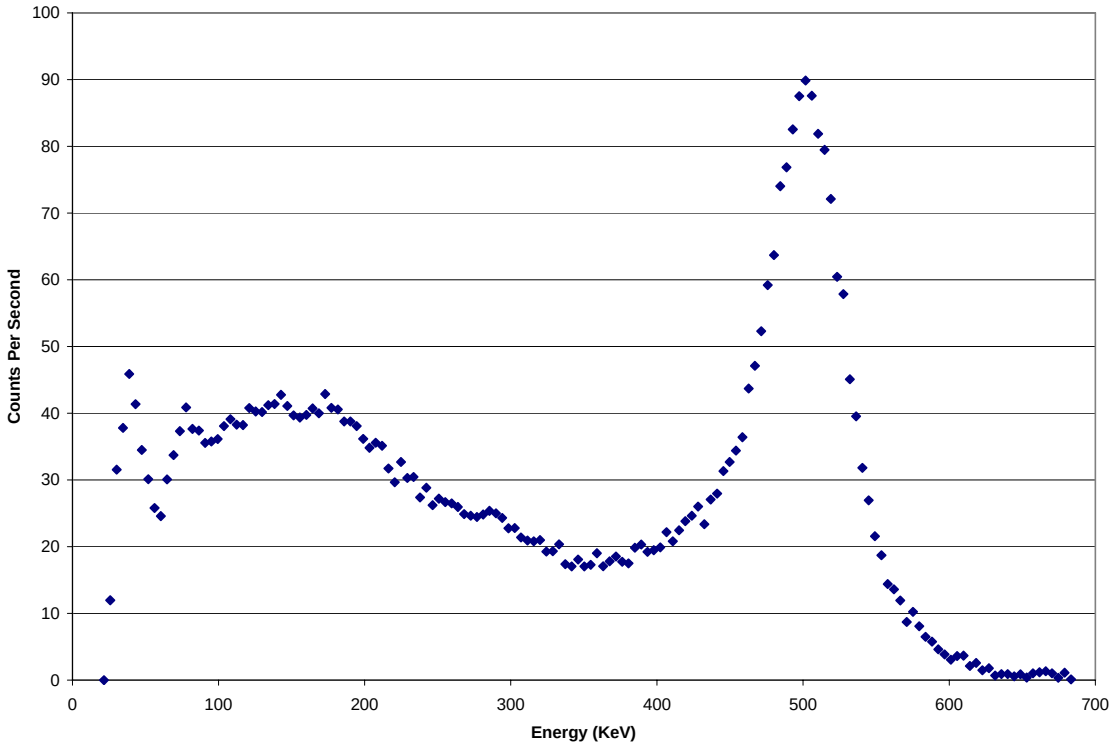

August 4, 2010 Outer Corridor Leaded Wall Patient Spectrum Measurement.

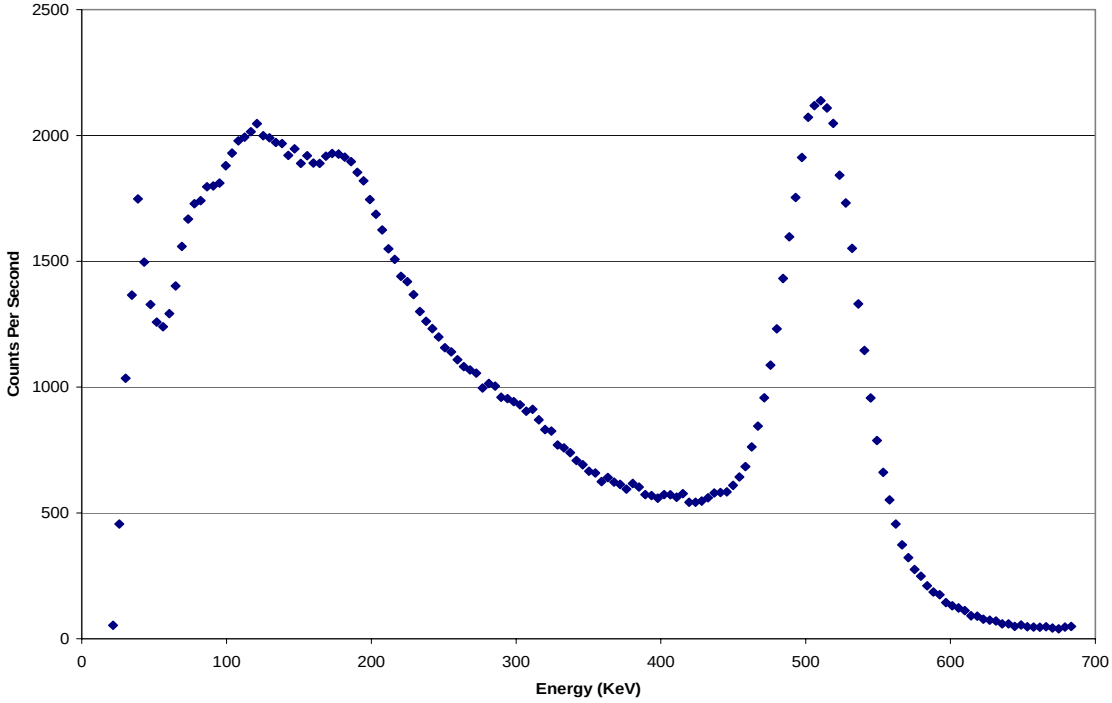

August 4, 2010 Inner Corridor Unleaded Wall Patient Spectrum Measurement.

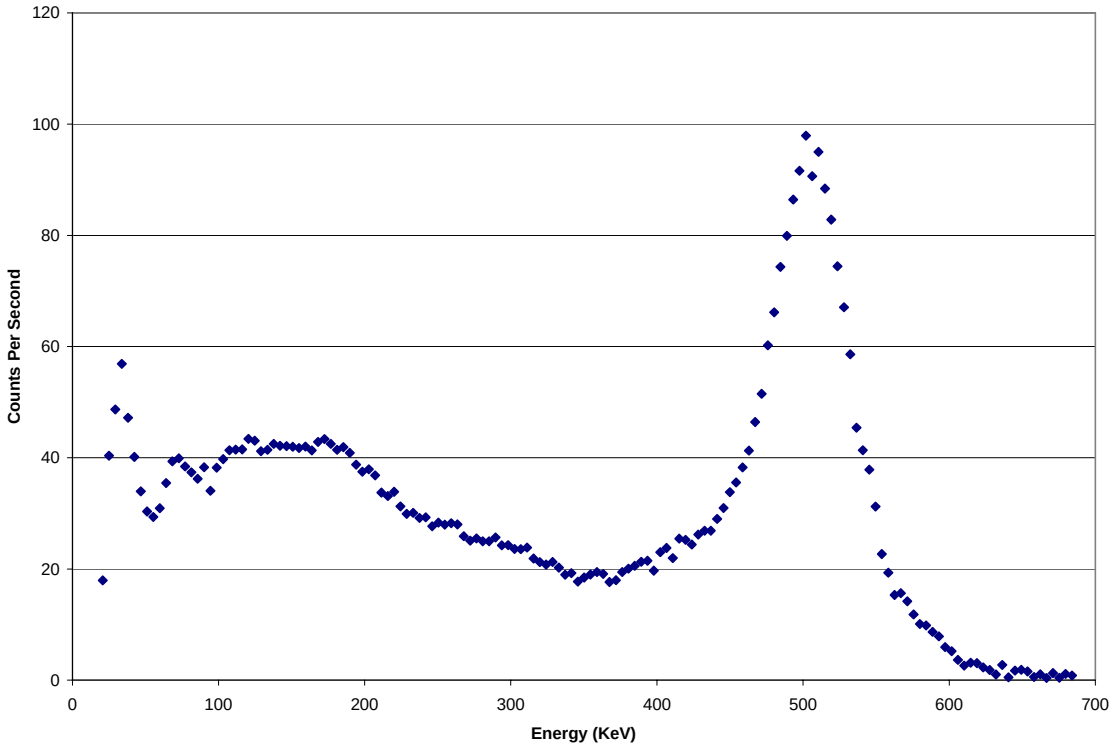

August 11, 2010 Outer Corridor Leaded Wall Patient Spectrum Measurement.

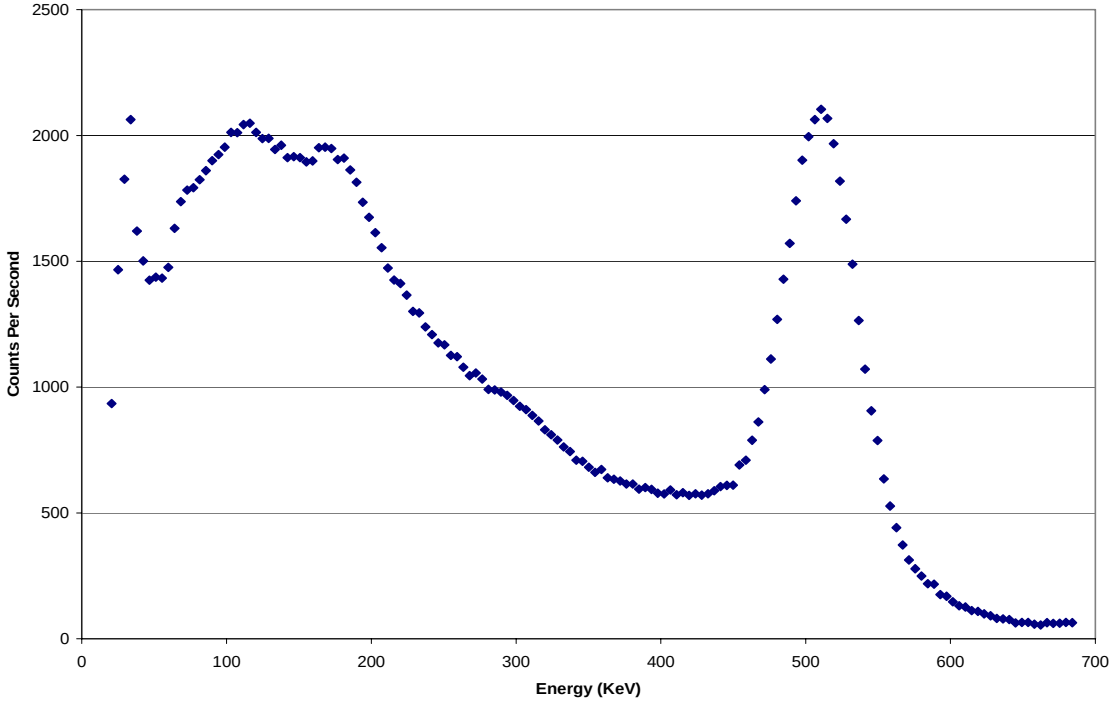

August 11, 2010 Inner Corridor Unleaded Wall Patient Spectrum Measurement.

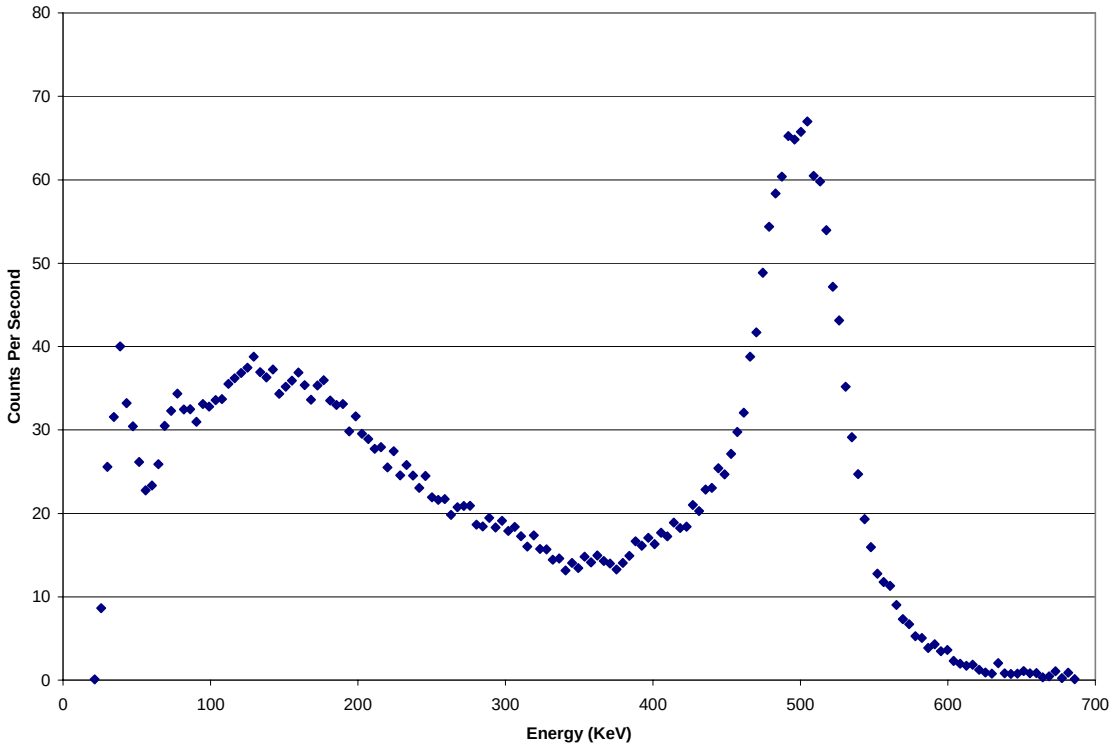

August 18, 2010 Outer Corridor Leaded Wall Patient Spectrum Measurement.

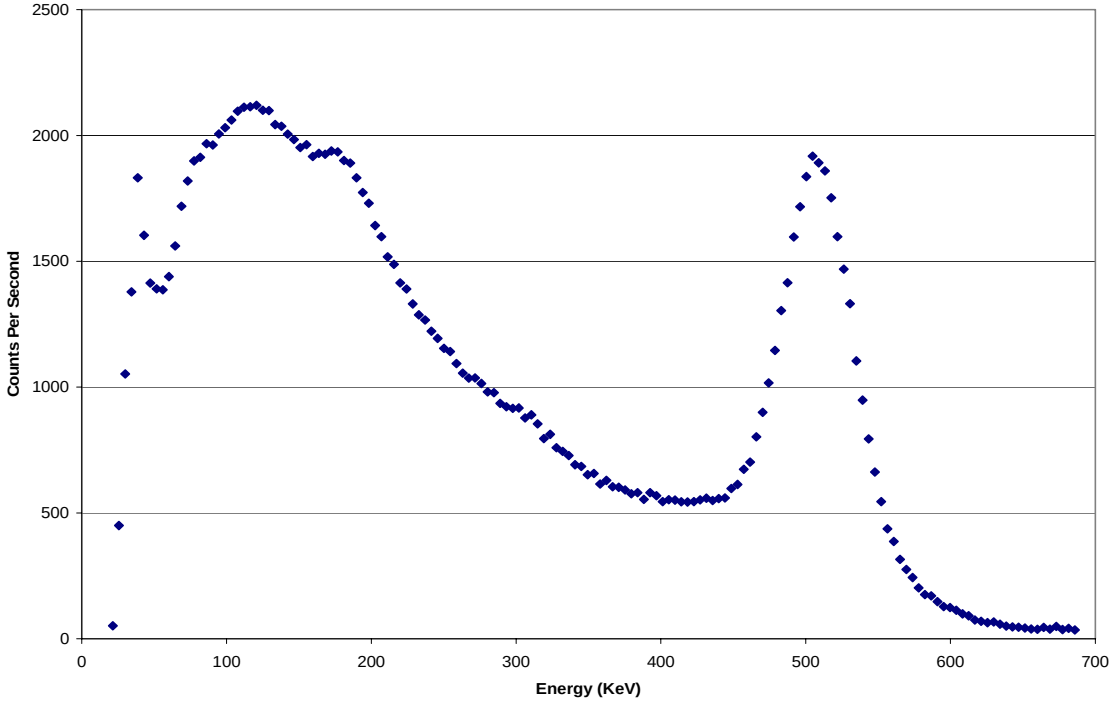

August 18, 2010 Inner Corridor Unleaded Wall Patient Spectrum Measurement.

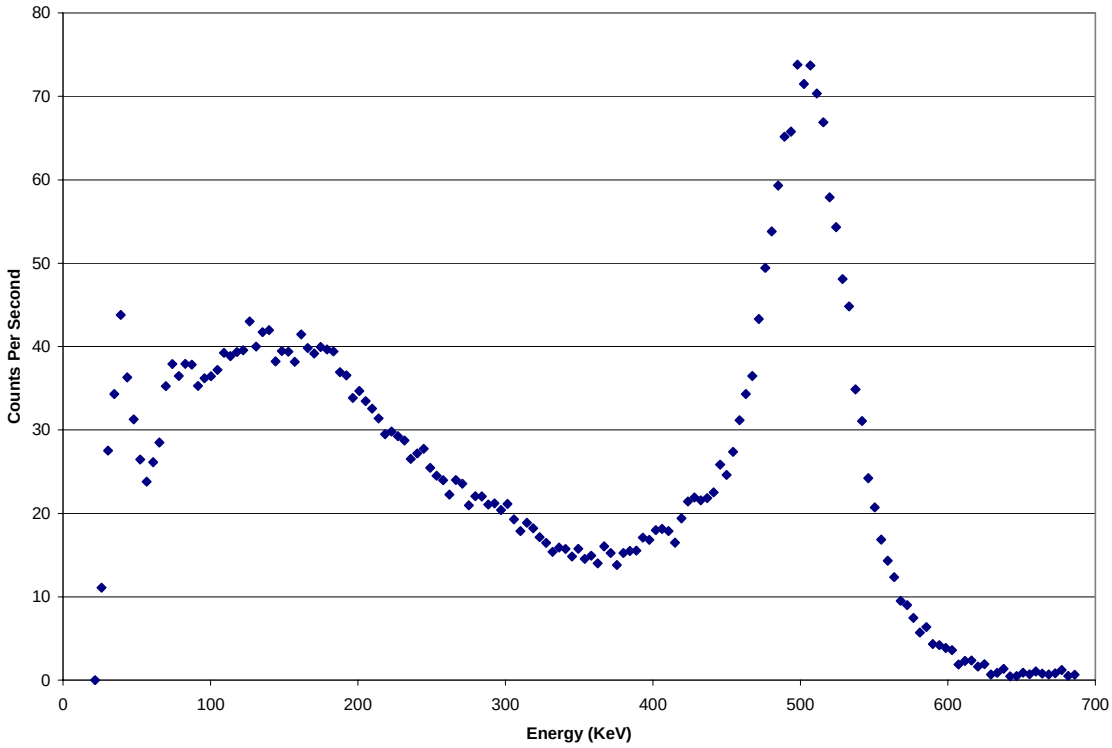

August 24, 2010 Outer Corridor Leaded Wall Patient Spectrum Measurement.

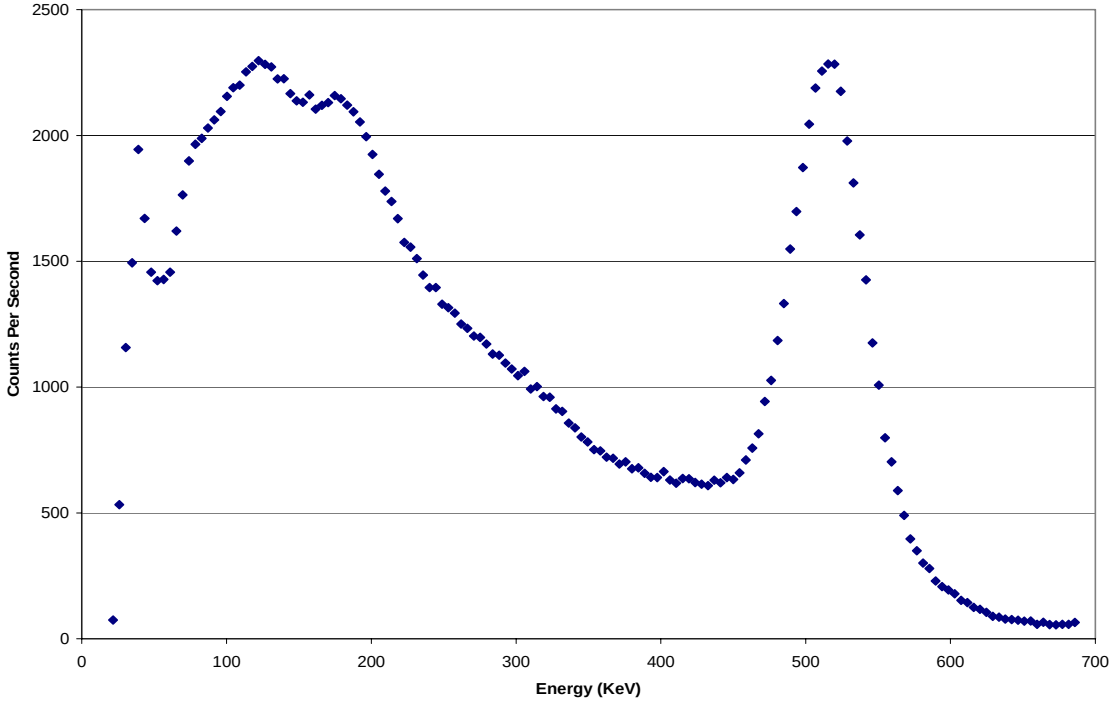

August 24, 2010 Inner Corridor Unleaded Wall Patient Spectrum Measurement.

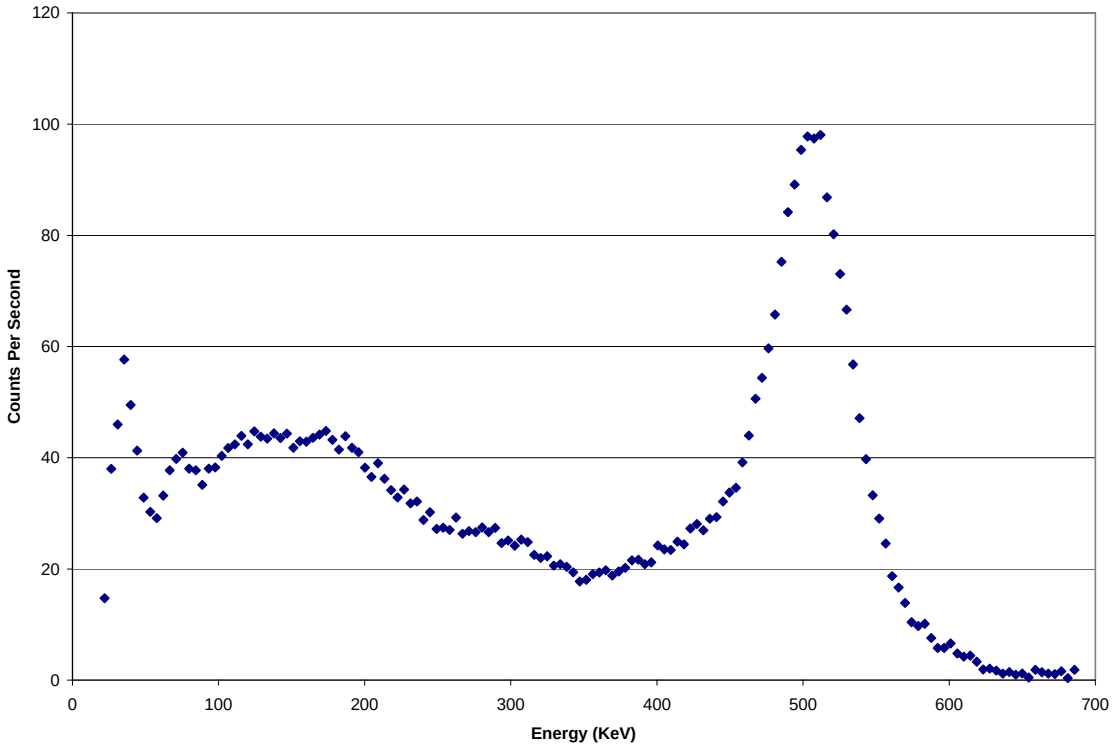

September 14, 2010 Outer Corridor Leaded Wall Patient Spectrum Measurement.

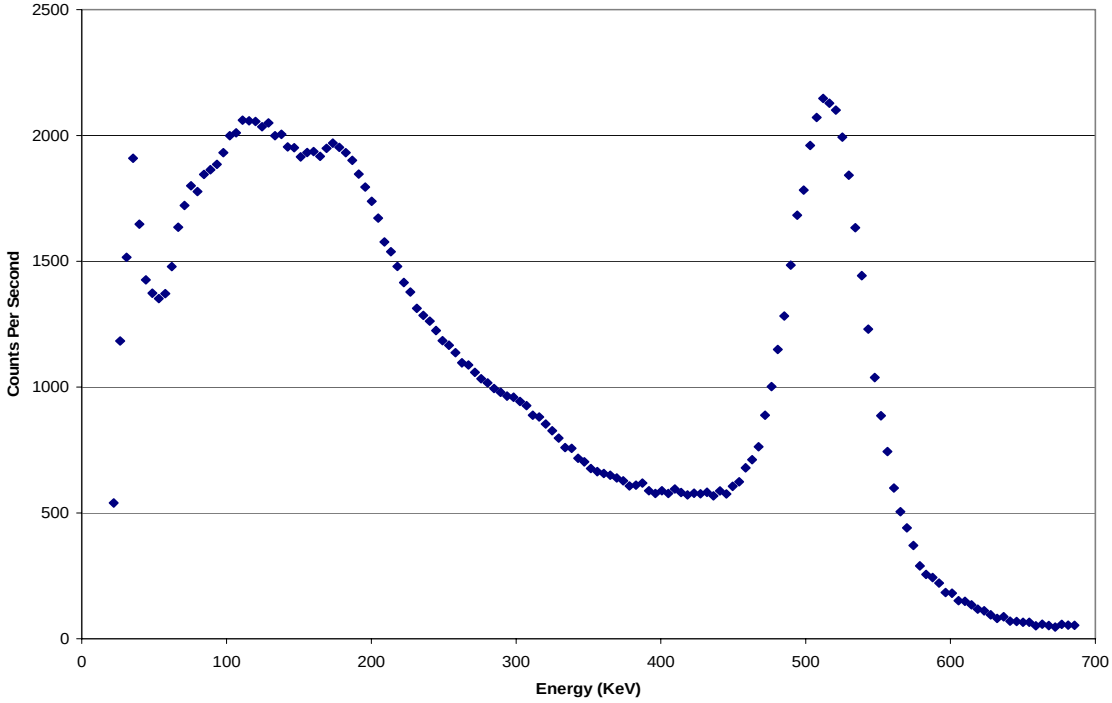

September 14, 2010 Inner Corridor Unleaded Wall Patient Spectrum Measurement.

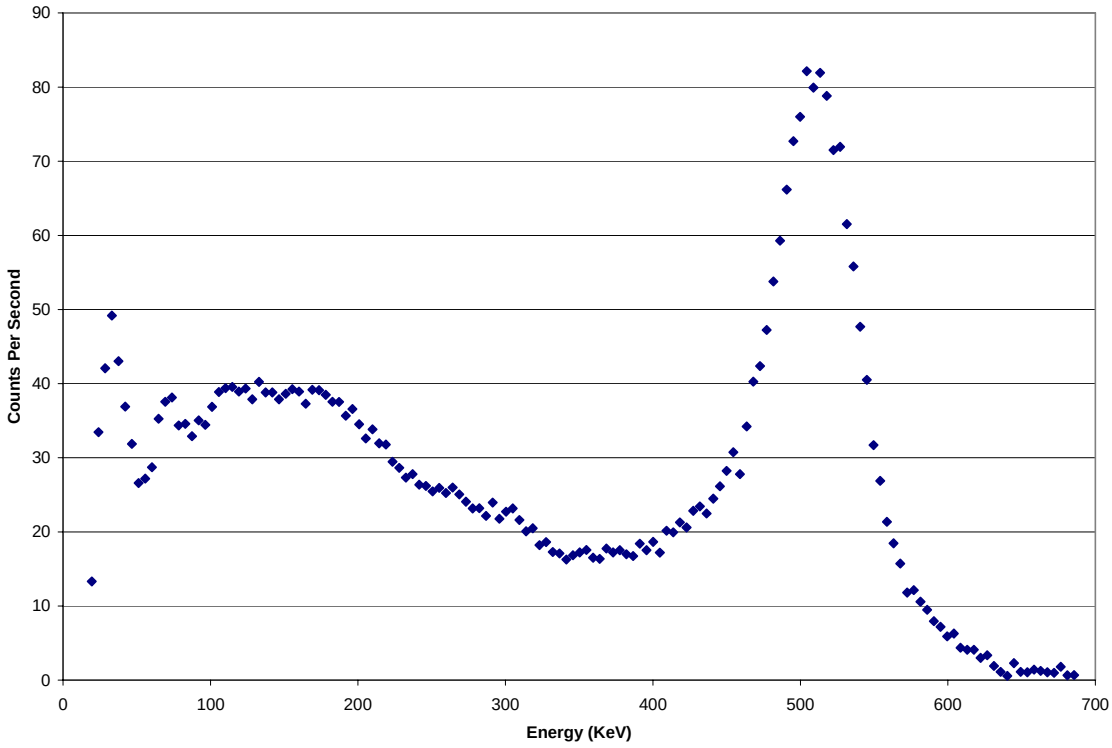

September 21, 2010 Outer Corridor Leaded Wall Patient Spectrum Measurement.

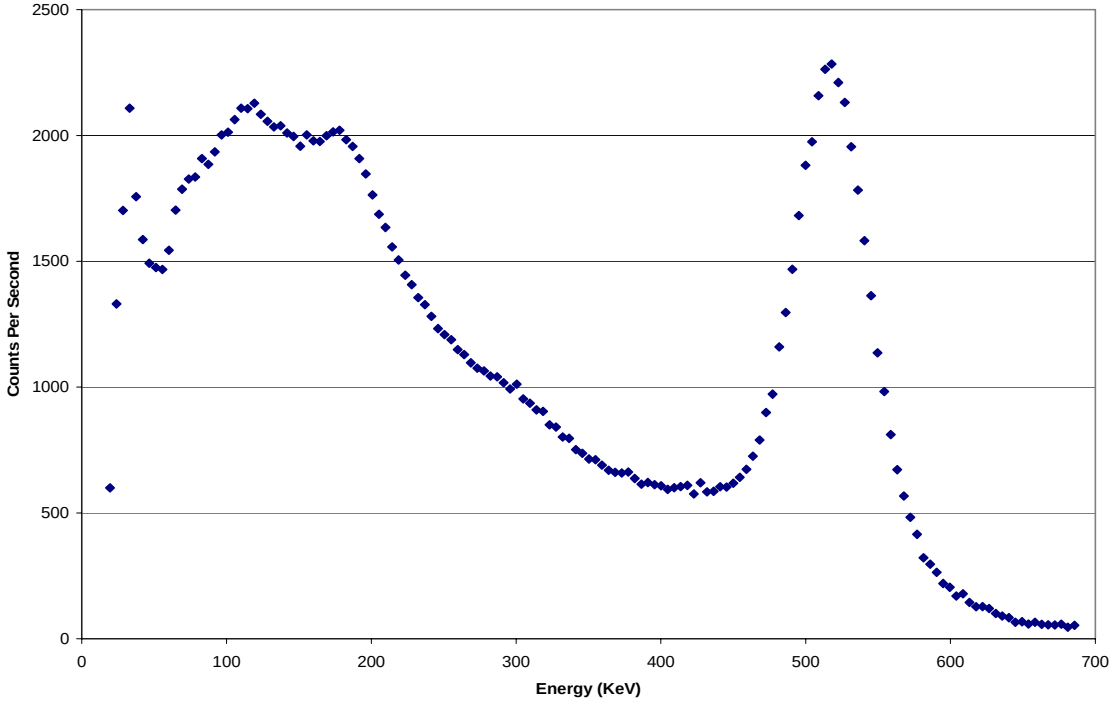

September 21, 2010 Inner Corridor Unleaded Wall Patient Spectrum Measurement.

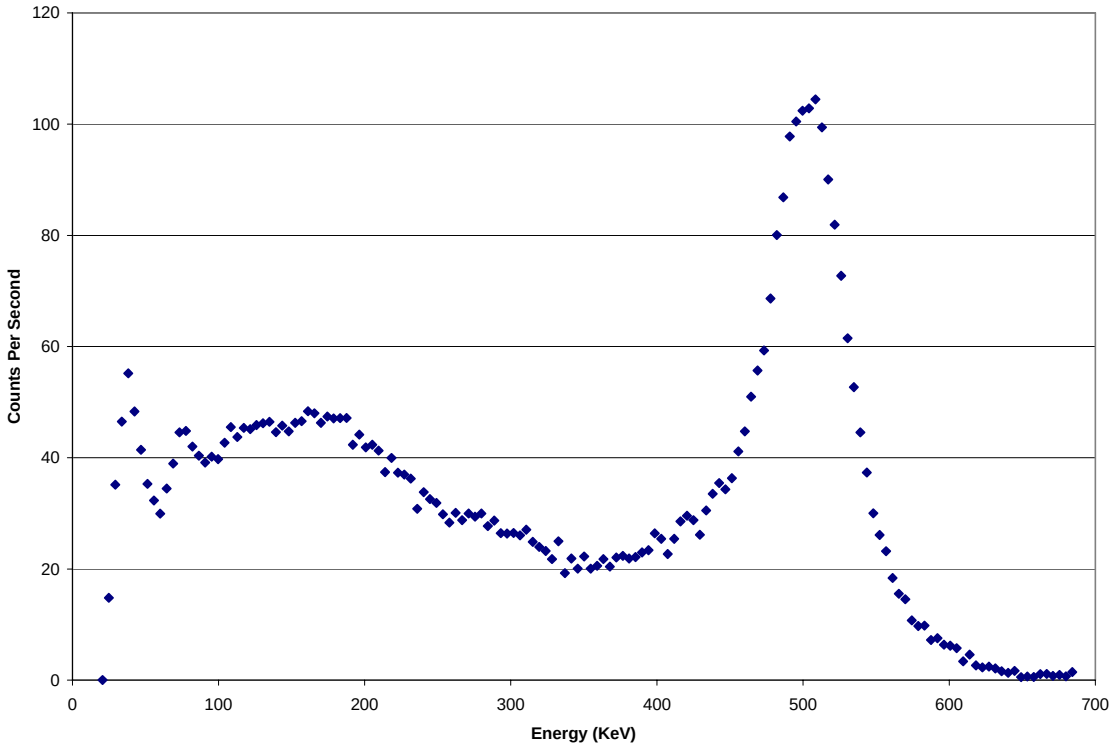

September 23, 2010 Outer Corridor Leaded Wall Patient Spectrum Measurement.

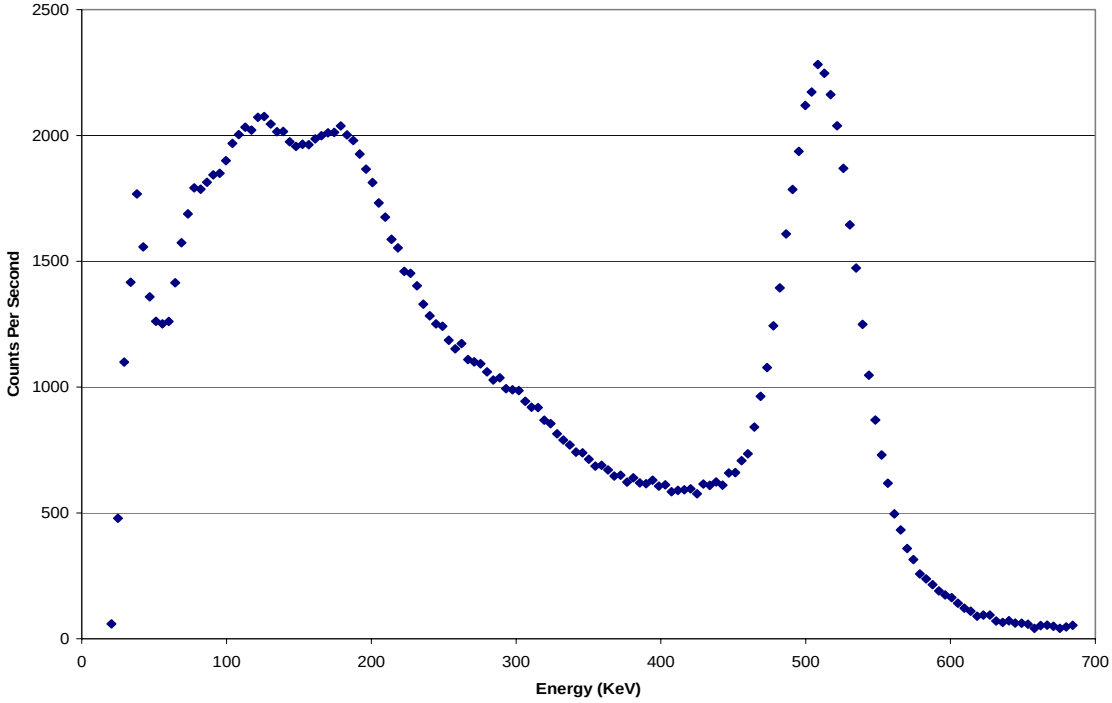

September 23, 2010 Inner Corridor Unleaded Wall Patient Spectrum Measurement.

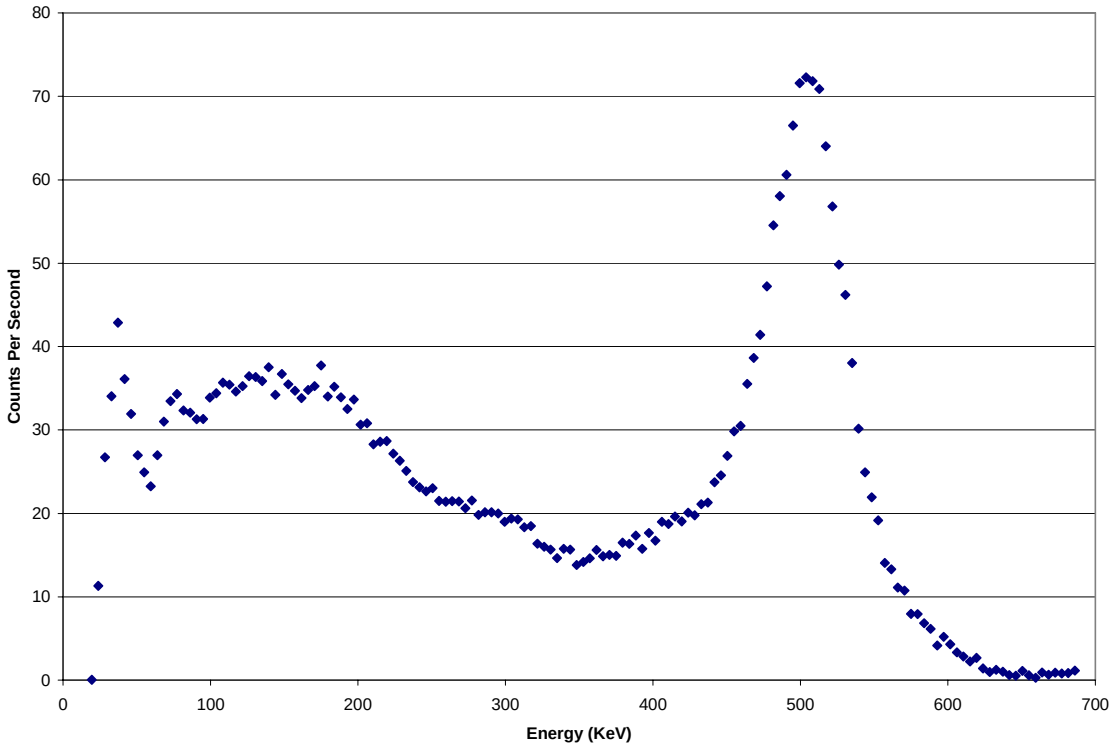

September 30, 2010 Outer Corridor Leaded Wall Patient Spectrum Measurement.

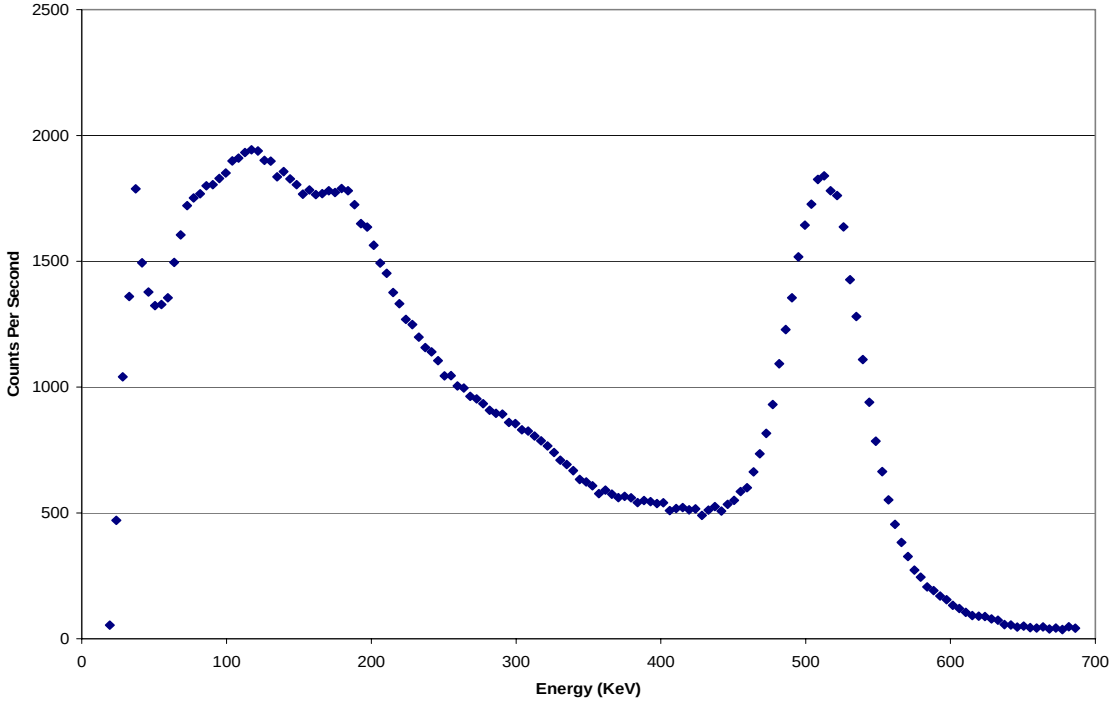

September 30, 2010 Inner Corridor Unleaded Wall Patient Spectrum Measurement.

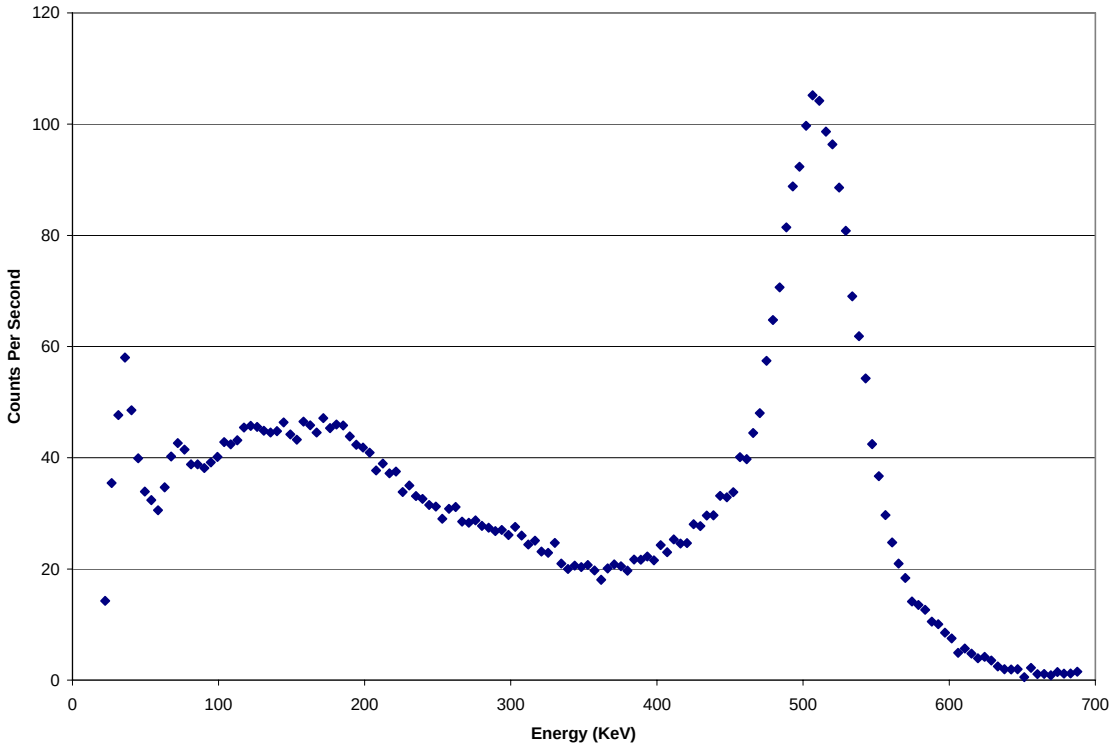

October 13, 2010 Outer Corridor Leaded Wall Patient Spectrum Measurement.

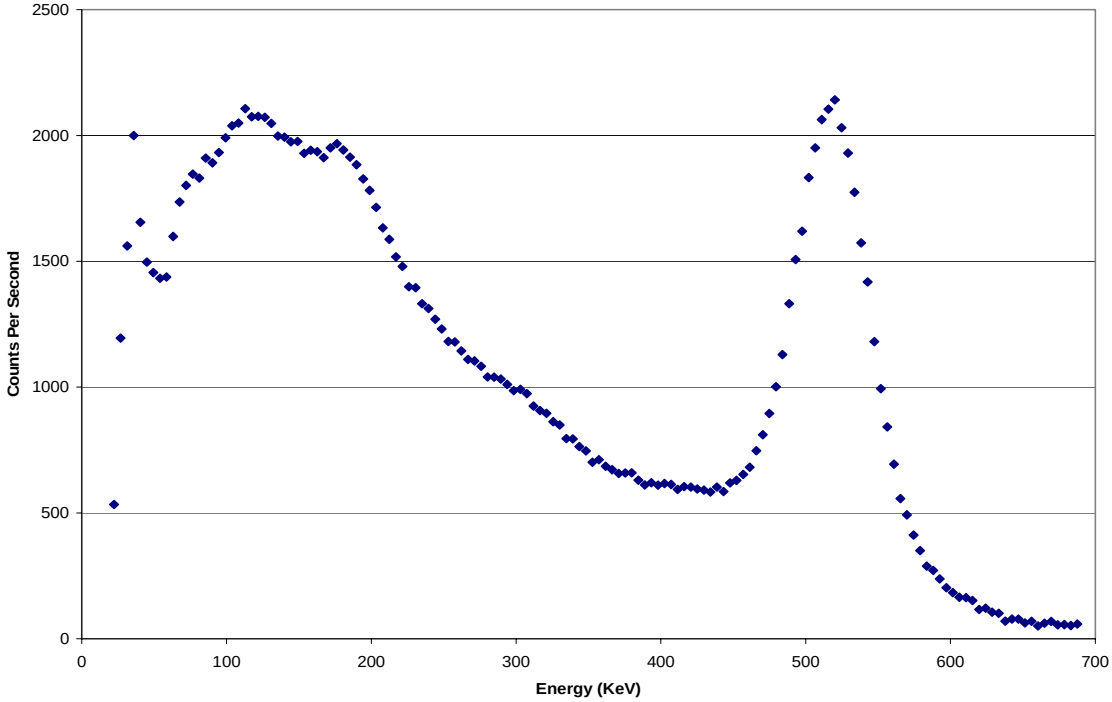

October 13, 2010 Inner Corridor Unleaded Wall Patient Spectrum Measurement.

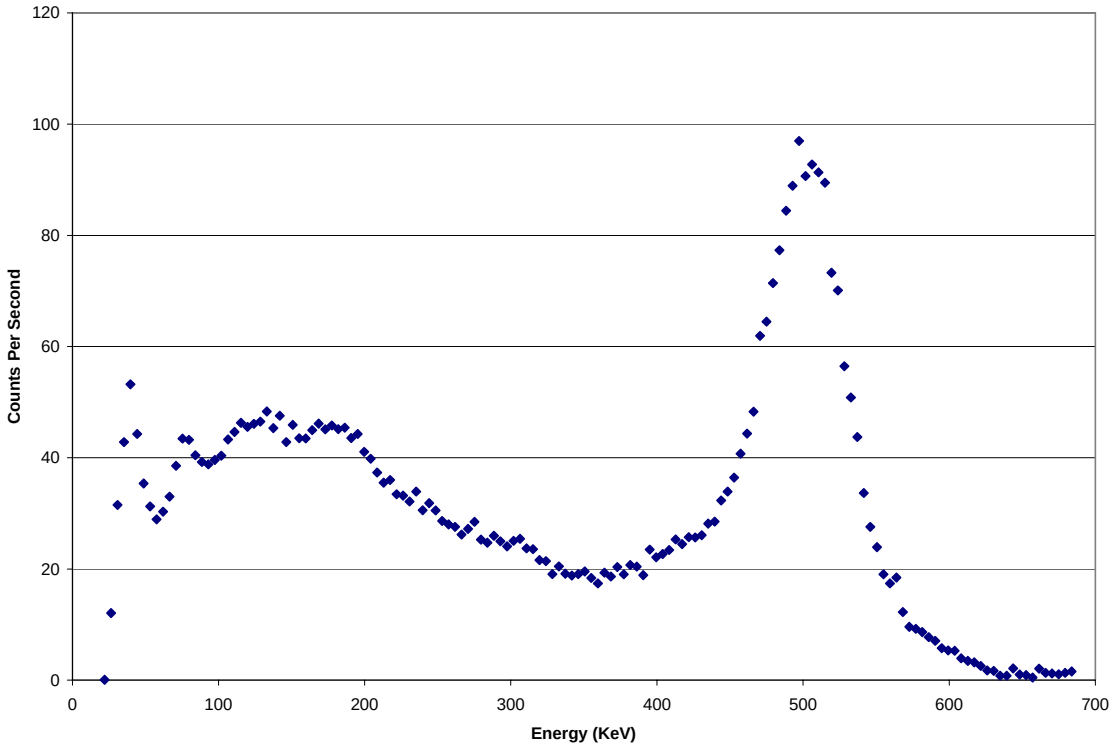

October 28, 2010 Outer Corridor Leaded Wall Patient Spectrum Measurement.

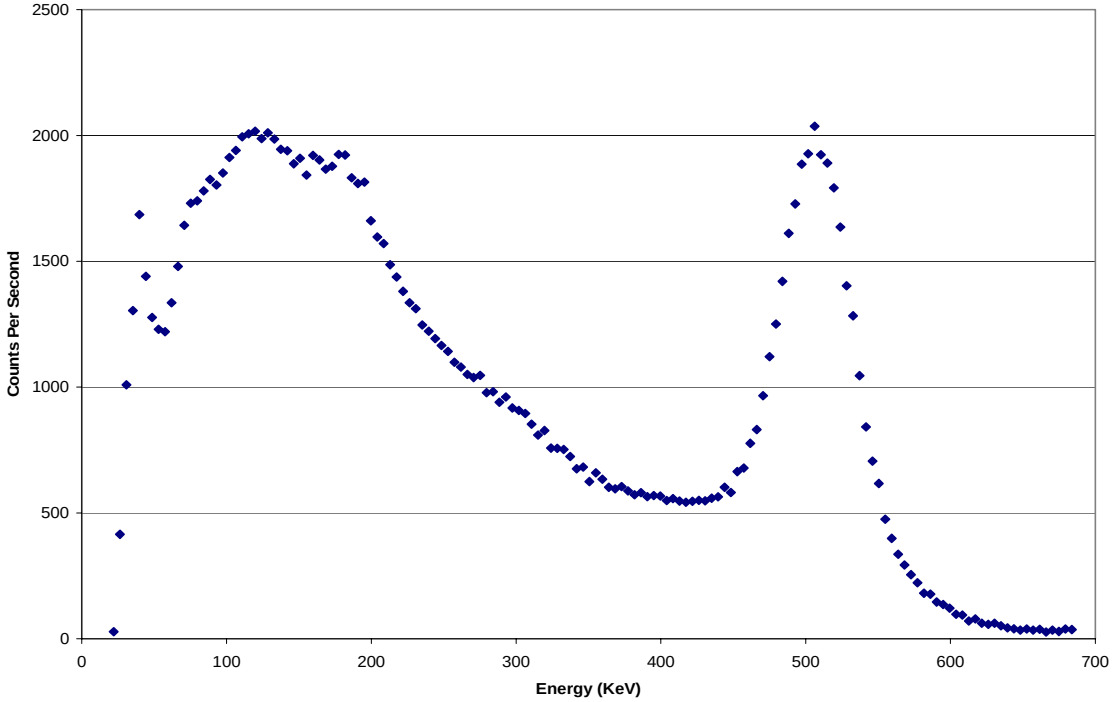

October 28, 2010 Inner Corridor Unleaded Wall Patient Spectrum Measurement.

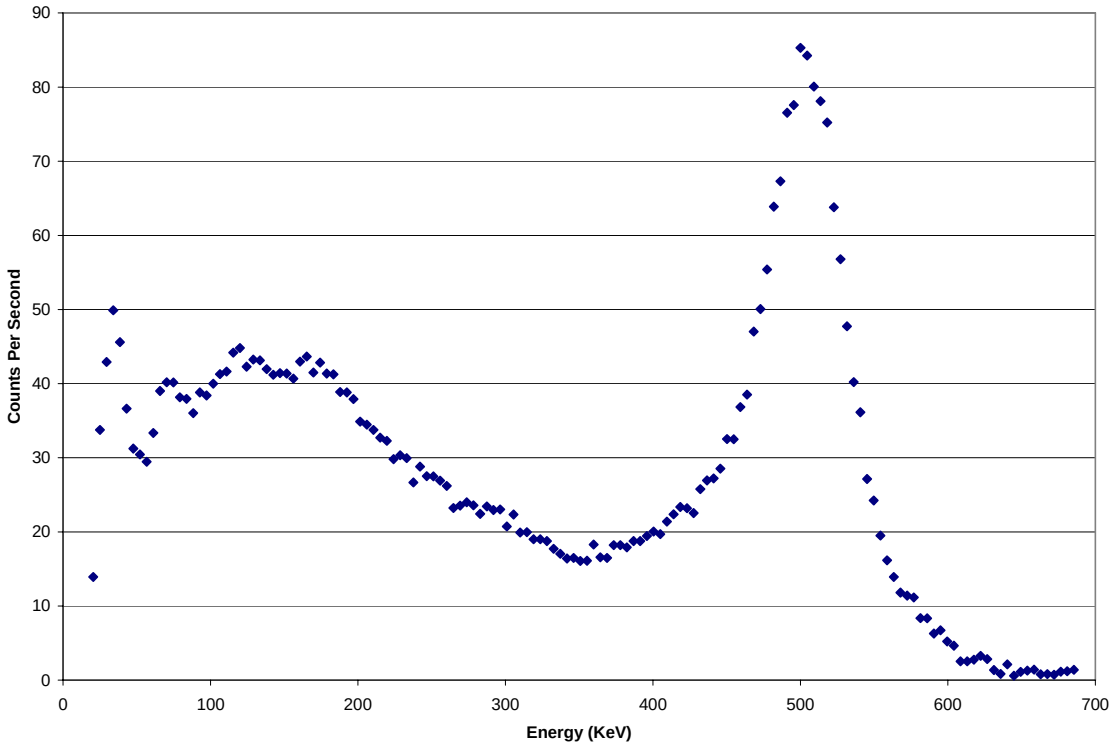

November 2, 2010 Outer Corridor Leaded Wall Patient Spectrum Measurement.

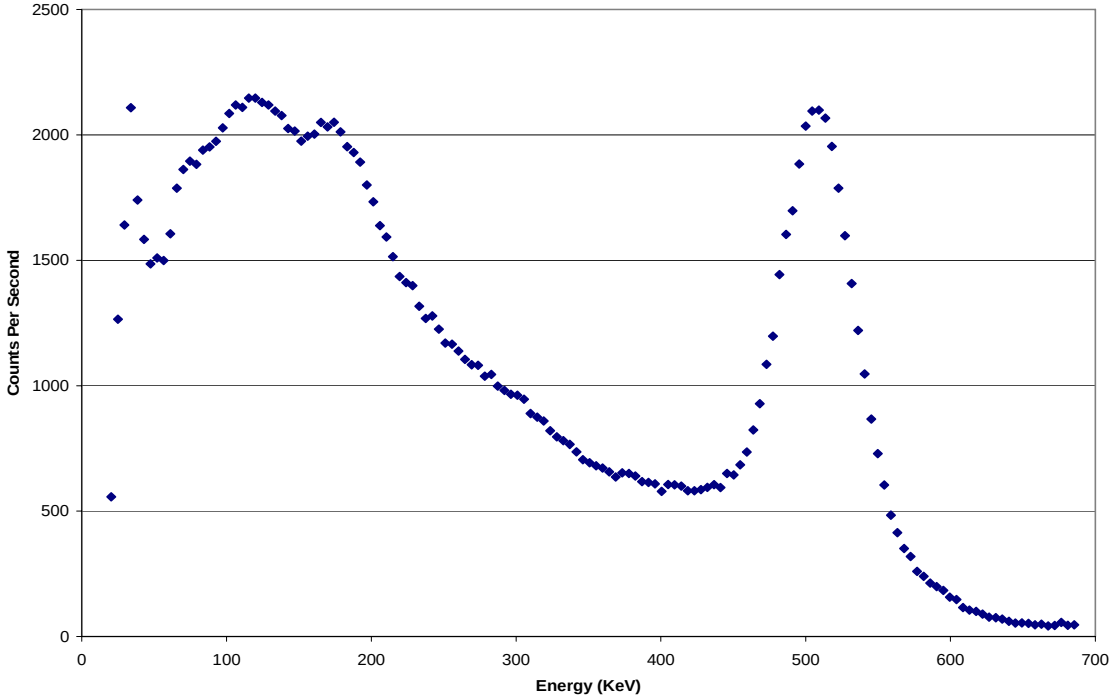

November 2, 2010 Inner Corridor Unleaded Wall Patient Spectrum Measurement.

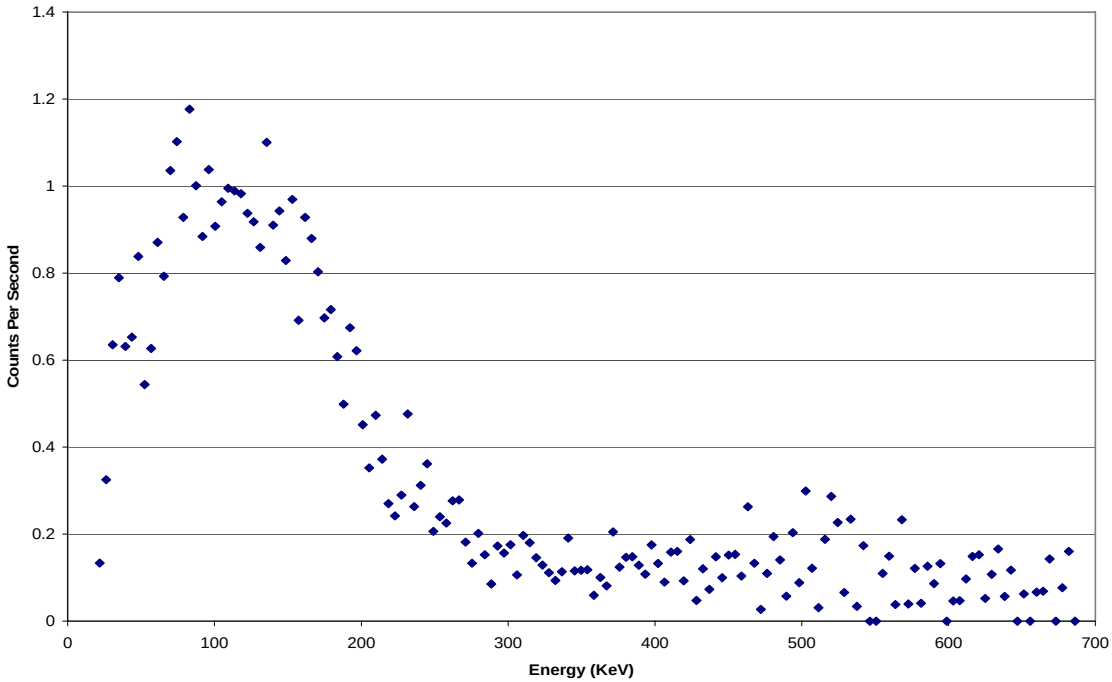

June 2, 2010 Background Spectrum Measurement Subtracted From Patient Spectra Measurements Made With a Patient on the Scanner.

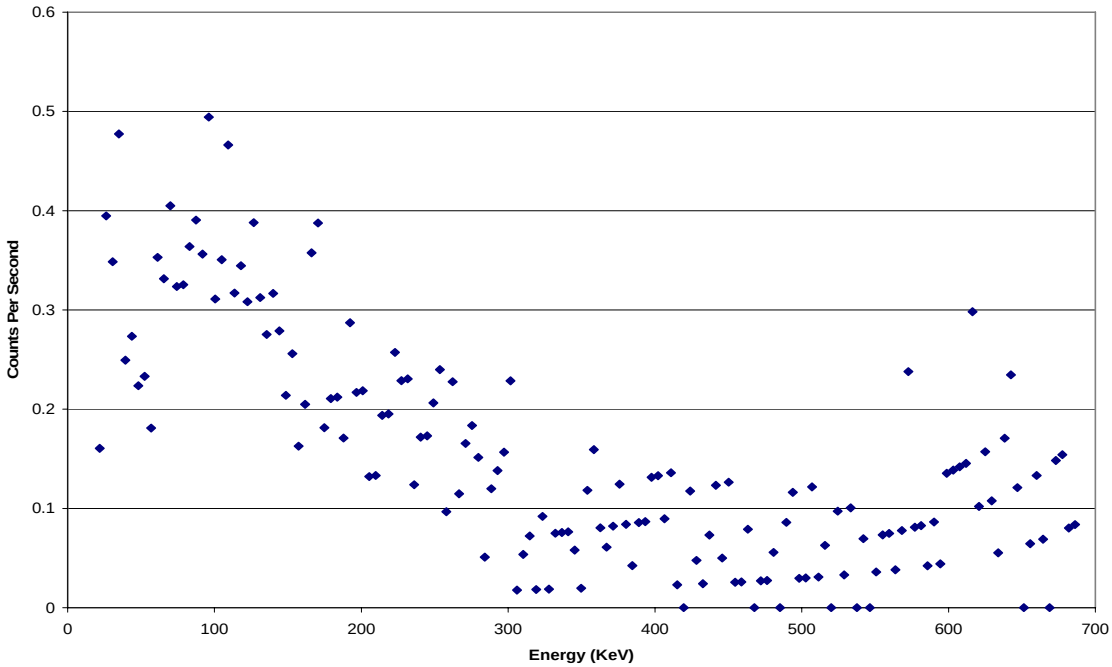

June 2, 2010 Background Spectrum Measurement Subtracted From Patient Spectra Measurements Made Without a Patient on the Scanner, and Also Subtracted From the July 7, 2010 Phantom Measurements.

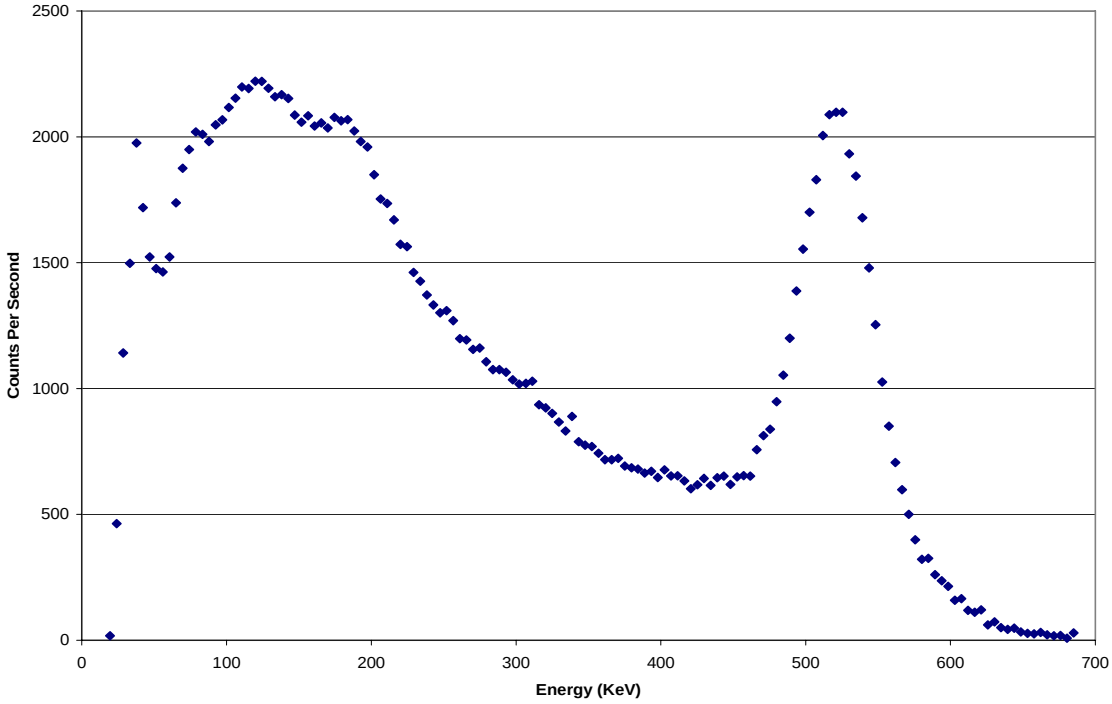

May 7, 2010 Inner Corridor Unleaded Wall Phantom Spectrum Measurement.

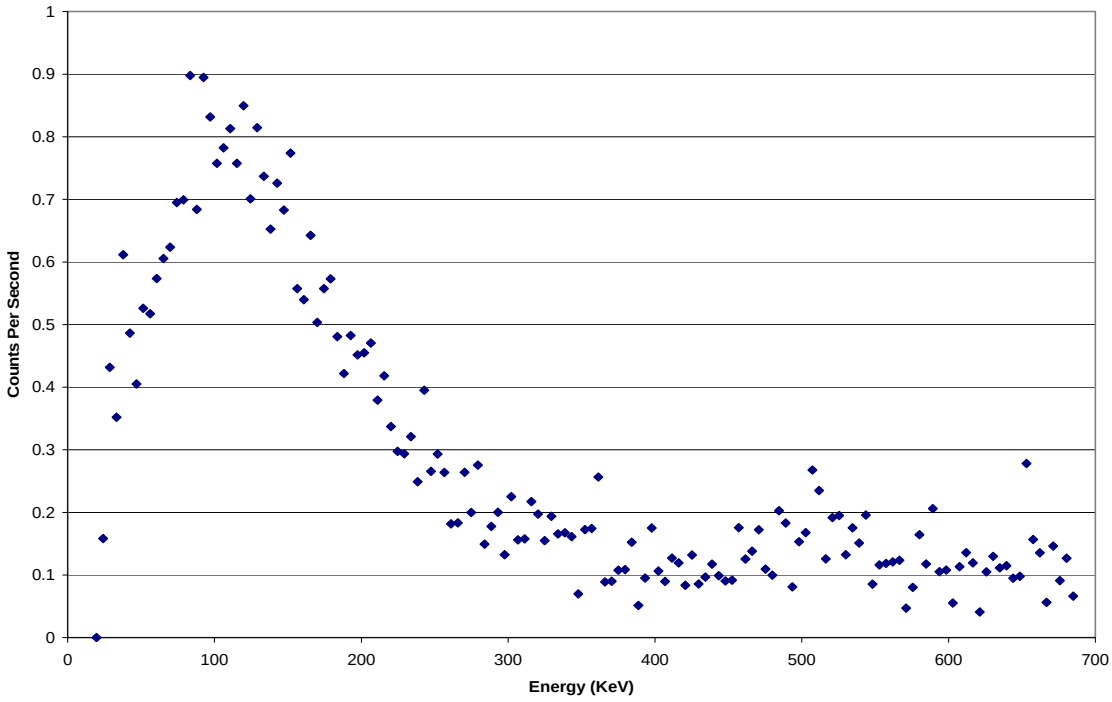

May 7, 2010 Background Spectrum Measurement Subtracted From May 7, 2010 Phantom Spectra Measurements, Made Without a Patient on the Scanner.

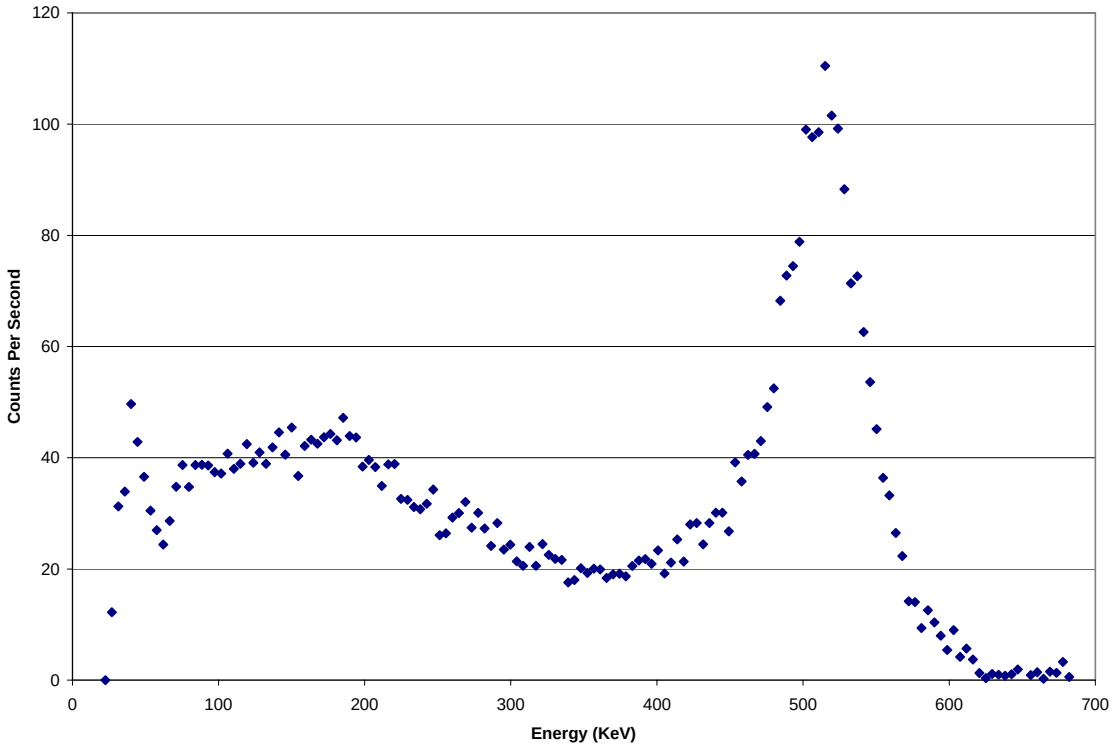

July 7, 2010 Second Outer Corridor Leaded Wall Phantom Spectrum Measurement.

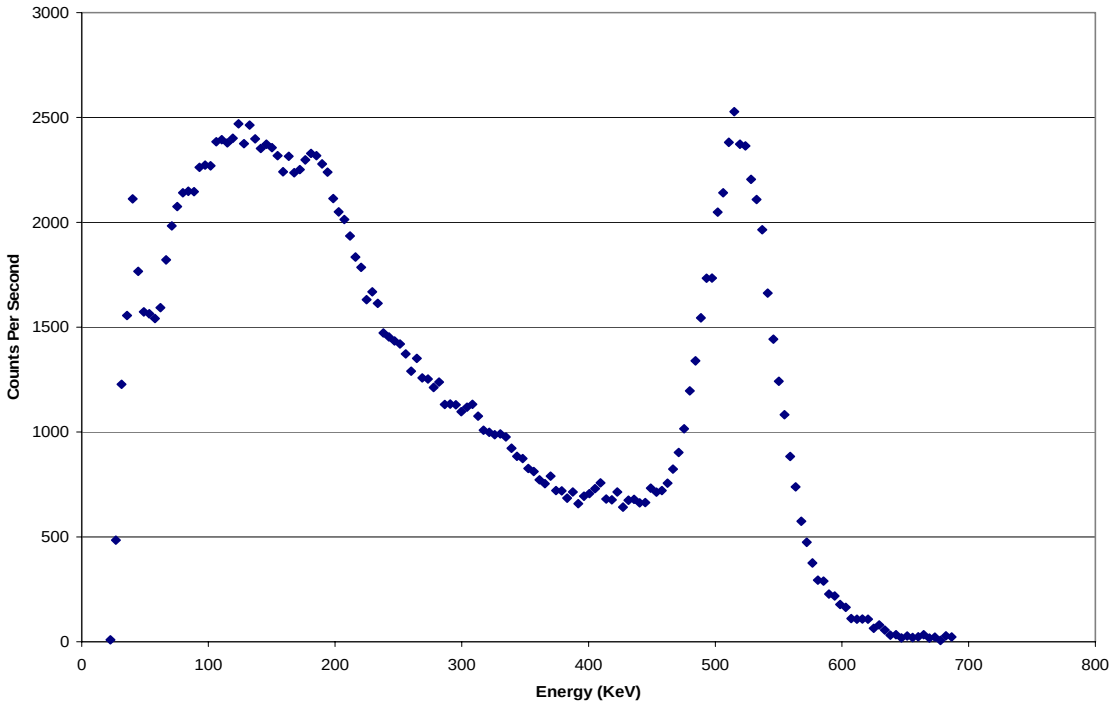

July 7, 2010 Second Inner Corridor Unleaded Wall Phantom Spectrum Measurement.

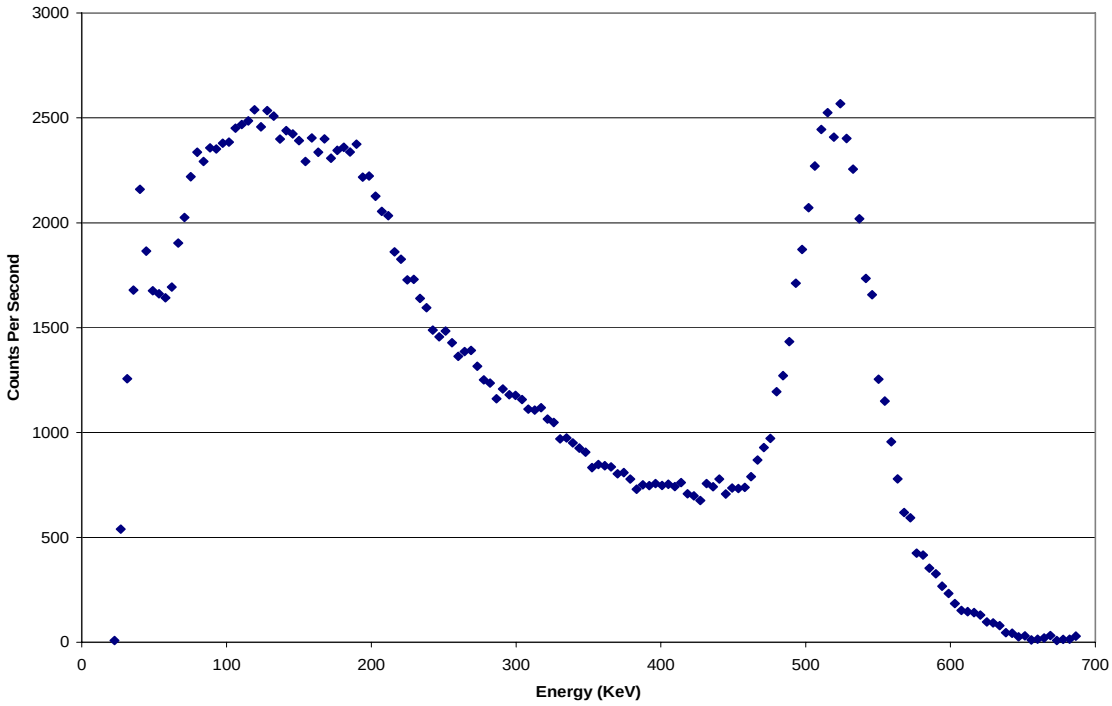

July 7, 2010 Inner Corridor Unleaded Wall Phantom Spectrum Measurement Made With the Sodium Iodide Detector Pointed Directly at the Phantom.

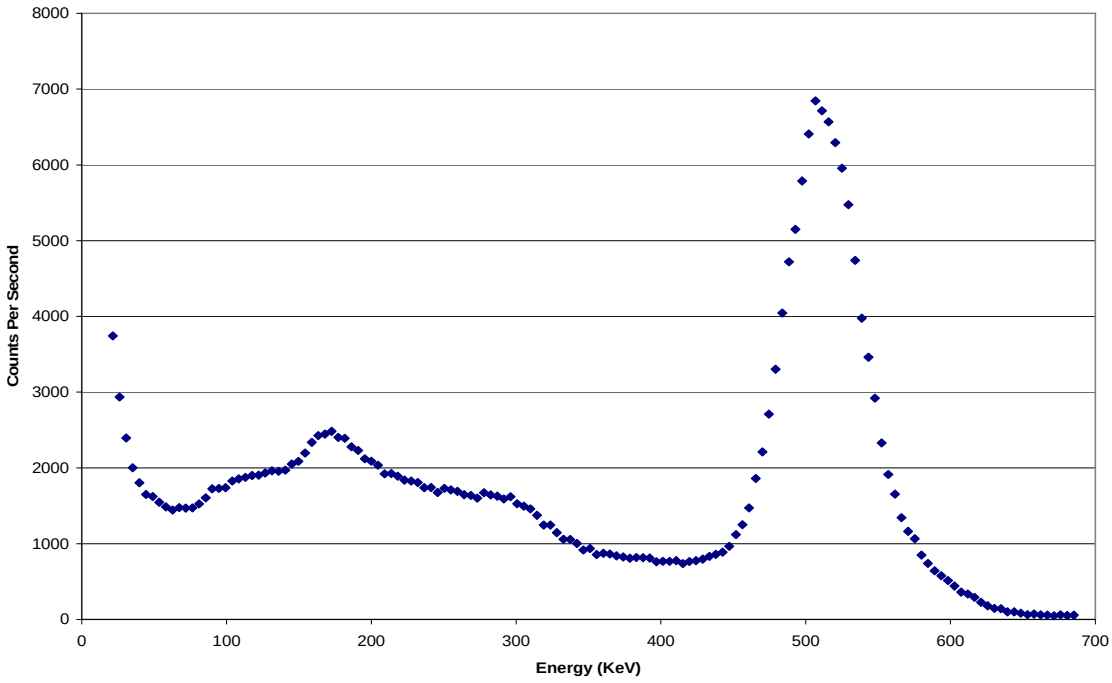

March 16, 2010 Second Inner Corridor Unleaded Wall Point Source Spectrum Measurement.

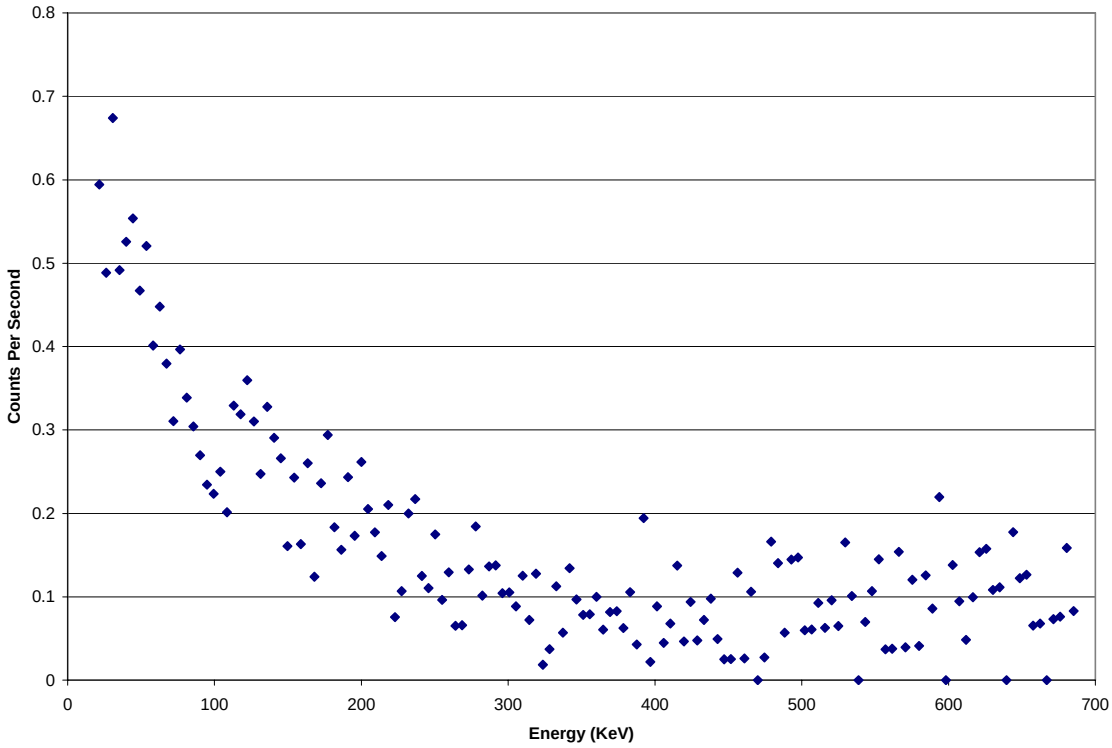

March 16, 2010 Background Spectrum Measurement Subtracted From March 16, 2010 Point Source Spectra Measurements, Made Without a Patient on the Scanner.